UNIVERSITY OF NAPLES FEDERICO II

School of Polytechnic and Basic Sciences

Department of Chemical, Materials and Industrial Production Engineering

XXXII Ph.D. Programme in

Industrial Products and Processes Engineering

Ph.D. Thesis

Effects of recycled powders on parts made by Selective Laser Melting Technology

Ph.D. Course Coordinator:

Prof. Eng. Giuseppe Mensitieri
Department of Chemical, Materials and
Industrial Production Engineering
University of Naples Federico II

Ph.D. Student:

Eng. Vincenzo Contaldi

Ph.D. Supervisor:

Prof. Eng. Antonino Squillace
Department of Chemical, Materials and
Industrial Production Engineering
University of Naples Federico II

Academic Year 2016-2017

CONTENTS

FIGURES INDEX

TABLES INDEX

INTRODUCTION

Among the additive manufacturing (AM) techniques for metals available today, the laser powder bed fusion (L-PBF) is the one that guarantees the highest dimensional accuracy and precision, compared to laser metal deposition (LMD) methods that, however, offer higher productivity and the possibility of repair applications. A drawback of most of PBF processes, in the case of both laser and electron beam melting, is that the build volume has to be entirely filled up to the height of the tallest object to be produced, even in the case of a single object [1]. Since not all the powder loaded into the build volume is melted to obtain the desired parts, it may be reclaimed for reuse. However, excess powder participates in the process so that its chemical-physical characteristics will inevitably evolve through reuse cycles [2]. Due to the high cost of metal powders and the critical role of feedstock characteristics with respect to quality assurance of both part and process properties, it is important to investigate and maximize the number of times powder can be reused for subsequent AM runs without causing an unacceptable decay of the mechanical properties of produced parts [3, 4]. Research in this field is fundamental to allow worldwide standards organizations, such as ASTM International and ISO, to develop the standards needed to foster additive manufacturing applications. Since the introduction of these technologies, producers and users of PBF, based on both laser and electron beam, systems have been involved in defining streamlined procedures for powder recycling and product certification for the most commonly offered materials.

Knowing that powders recycling is intensively under investigation, this PhD thesis proposes an experimental investigation of two recycle strategies, chosen according to an academic and industrial point of view. In order to investigate and understand the mechanisms and the effects of recycling process, the experimental activities reported in this work refer to powders, tensile and fatigue samples manufactured using Selective Laser Melting technology and employing four of the most widespread and studied alloys:

- *AlSi10Mg aluminum alloy*
- *Ti6Al4V titanium alloy*
- *PH1 (15-5 PH) stainless steel*
- *GP1 (17-4 PH) stainless steel*

CHAPTER 1 – ADDITIVE MANUFACTURING

Additive Manufacturing (AM) is defined as "a process of joining materials to make objects from 3D model data, usually layer upon layer, as opposed to subtractive manufacturing methodologies. Synonyms: additive fabrication, additive processes, additive techniques, additive layer manufacturing, layer manufacturing, and freeform fabrication", according to ASTM F2792.

Unlike traditional manufacturing processes such as turning and milling that produce parts by removing unwanted material from a larger piece, Additive Manufacturing processes creates unique components layer by layer, one layer at a time.

At the very beginning, 3D Printing Processes were dedicated to polymeric materials due to their capability to melt and cool down easily. As expected, these parts had (and still have) no mechanical properties aerospace/mechanical industry could accept. For this reason, 3D printing of polymeric materials only boosted the rapid prototyping field. New shapes were then possible, and a fast creation of plastic model allowed team to see (and touch) their digital 3D models. 3D printed became soon an irreplaceable way to create 3D prototypes and physically see ideas and projects.

Rapidly, 3D printing technologies involved metallic materials: the process behind totally changed. From a simple extrusion and deposition of polymer via a heated orifice to laser tools, ultra-precise platforms and inert gases: in fact, melting (or sintering) a metal's powder, a 3D printing process requires a laser or an electron beam. These techniques can produce complex parts with astonishing internal features that cannot be created with any other traditional technique. The most important advantage is that these features are obtained without tooling, creating a direct link from the digital design to the real production.

1.1 BENEFITS AND CHALLENGES

Additive Manufacturing can competitively produce low-volume and customized products, with intricate internal lattice features and complex external geometries. The growth of the application fields for additively manufactured parts has been encouraged by the following benefits [5 -8].

- **Design freedom and flexibility.** AM offers the possibility of creating complex objects and shapes, that are difficult, or even impossible, to obtain with conventional technologies. Moreover, the additional levels of product complexity do not add cost to production. The possibility to realize products with fewer and more complex parts, rather than a large number of simpler parts, can be associate to less time and labor required for assembling the product, contributing to a reduction in manufacturing costs.
- **Structural lightweighting.** A structural member can be built with the same functional specifications of the conventionally manufactured parts, but with less material. This topic has significant implications on reducing material costs and improving energy efficiency in transportation.
- **Supply chain efficiencies.** The customers can print the items in remote locations, taking advantage of the widespread availability of internet. The ability to produce parts on site without the need for tooling and setup, combined with the potential reduction of the costs for storing, moving and distributing raw materials, mid-process parts and end-usable parts, can be considered a topic for new solutions in supply chain management [9].
- **Reducing time to market.** Time to market is expected to shrink due to shorter design and prototyping cycles and the elimination of tooling and setup time for new products. The freedom to design and redesign prototypes and parts without increasing production time and cost, enables a more fluid development process.
- **Mass customization.** The ability to employ multiple designs on the same machine could enable the manufacturing industry to move from mass production in factories to mass customization with distributed and local manufacturing. The exploitable materials range, from plastic to metal to even human tissue, offers the possibility to create a nearly infinite variety of products that can be produced according to exact customer specifications.
- **Environmental sustainability.** The elimination of production steps, the production of lighter parts, with substantially lower use of material, the production decentralization and the imposition of few constraints on product design make AM a tool for mitigating environmental impact compared to other

manufacturing processes that consume significant amounts of energy and produce great industrial waste [10,11].

The transition to a robust manufacturing production for an eventual widespread commercial exploitation requires large-scale changes and investments to overcome some key technical barriers [12, 13].

- **Standards development.** Developing standards is crucial for the increasing diffusion and adoption of the technology. New standards would provide a foundation for creating products compliant with well-defined specifications and compatible with products provided by different suppliers. In addition, they would ensure the safety, reliability and quality of AM processes and products. Standards are also needed for software compatibility across AM machines: there is a number of proprietary formats that do not work well together, hence slowing and limiting production. Another area that would benefit from standards development is material property data generation: measurement (metrology) capacity, closed-loop and adaptive control systems, as well as new sensors for build properties, such as shape and surface finish, are severely lacking. Despite the foundation of the Committee F42 in response to those requests, the AM industry has identified many additional needs for standards that will take much effort and time to develop.
- **Material characterization and development.** Despite the recent progress in material characterization and development, several issues, including a limited selection of materials, inconsistent production quality and high cost, are still present. Only a fraction of the materials used in conventional manufacturing is compatible with AM. Most processes use proprietary polymers that are not well characterized and that often exhibit weaker and not uniform part strength, if compared to the materials used in traditional manufacturing. The additively manufactured metal parts have physical properties that can be quite different from conventional wrought or cast metals: they may, for example, lack full density, which can compromise fracture toughness and fatigue properties, due to porosity, or partial delamination, which can act as crack initiation sites in the material.

- **Equipment and processes.** Establishing AM as a mainstream technology is contingent upon overcoming significant constraints in equipment and processes. Although the prices of industrial machines are decreasing and the capabilities of software and scanning devices are improving, other limitations are less likely to be surmounted soon. The physics of layering and curing, for example, imposes some limits on the process speed and the issue of minimum wall thickness still remains a fundamental restraint that is unlikely to be overcome without a significant technological advancement. The outlined technological barriers include:
  - high costs of equipment and materials in comparison to those used in conventional manufacturing;
  - product fabrication speeds, significantly slower than that related to mass production processes;
  - inherent trade-offs between product size, accuracy and speed (larger surfaces entail lengthier production time, while accelerated production processes may result in parts with unknown and unpredictable properties);
  - significant geometric and property variation between identical products build on different machines, leading to a lack of repeatability;
  - unreliable machinery and inconsistent product quality, particularly with regard to part accuracy and surface finishing;
  - closed architectures which preclude researchers from making meaningful changes to processing conditions;
  - lack of hardware and software necessary for simple and effective multi-material deposition.

1.2 METAL ADDITIVE MANUFACTURING OVERVIEW

Current metal additive manufacturing processes include indirect methods such as Binder Jet processes and Selective Laser Sintering, and direct methods such as Selective Laser Melting, Electron Beam Melting, and Laser Engineered Net Shaping. Indirect methods require post-processing such as Hot Isostatic Pressing to produce parts of density greater than 90% while direct methods can typically produce parts with more than 90% density

with optimized process parameters. In indirect methods, metal powders are either partially solid-state sintered together or a low melting point binder is used to bind metal particles together to produce a preform. Post-processing operations such as binder removal, sintering, or liquid metal infiltration are used to obtain greater than 90% build density.

The powder bed process is now entering a stage of technology maturity and is currently the most common metal 3D printing systems for production of engineering components. Current systems of this process use thermal energy to melt and fuse material through manipulation of a melt pool created by laser or electron beam coupled into metal powder as heat. The resulting structures, morphology, and microstructures of printed materials depend highly on the thermal-physical and heat-transfer processes during the micro-welding event These processes use fine powders as the starting material which can pose health and safety concerns especially when reactive metal powders such as aluminium or titanium are used. Because of the heat melt-fusion nature of this technology, the part building process takes place under controlled environment of inert gases or vacuum to prevent excessive oxidation, beam scattering in the case of electron beam melting, and process hazards.

In this work of thesis, the attention was focused on a powder bed fusion technology.

1.3 POWDER BED FUSION

In the Powder Bed Fusion (PBF) processes, a roller (or rake, or blade) spreads a thin layer of powder from a supply bin over the build platform. In some cases, a catch bin for exceeding powder may be present on the opposite side of the platform.

The powder bed is in an inert atmosphere or partial vacuum to provide shielding of the molten metal against oxidation or other kinds of contamination.

The energy source (laser or electron beam) passes through the scanner, programmed to move in a plane parallel to the build platform. Depending on the source and the power level of the system, the powder layer is melted or sintered into the desired shape. The raster scanning of the surface is performed according to certain possible paths, called scanning strategies, generally provided by the AM equipment producers. Once the layer is completely exposed, the platform descends by an amount equivalent to the powder

layer height, the next layer of powder is spread over the work area and the melting/sintering is repeated.

These processes inherently require some supports, realized with the same material of the parts to be produced, to avoid the collapse of the molten material in case of overhanging sections, to dissipate the heat developed during melting process and to prevent distortions due to residual stresses within the material. Supports can be generated and modified during the pre-processing phase and they have to be removed by machining operations during the post-processing phase. After support removal, the part may undergo several post-processing treatments like shot-peening, polishing, lathing or milling, depending on the production requirements.

Once the printing phase is completed, parts are usually subjected to heat treatment before supports removal and finishing, in order to relieve residual stresses.

Selective Laser Sintering (SLS), Direct Metal Laser Sintering (DMLS) from EOS GmbH, Selective Laser Melting (SLM) from Renishaw and SLM Solution, and LaserCUSING from Concept Laser GmbH are some of the PBF technologies which use a laser beam for powder melting. Conversely, Electron Beam Melting (EBM), from ARCAM, is the only PBF technology that uses an electron beam as energy source.

CHAPTER 2 – DIRECT METAL LASER SINTERING TECHNOLOGY

The basic principle of the DMLS is to fabricate near net-shape metal parts directly in a single process by using a high-power laser beam to sinter the metal powder layer-by-layer. A schematic diagram of DMLS is shown in Figure 1.

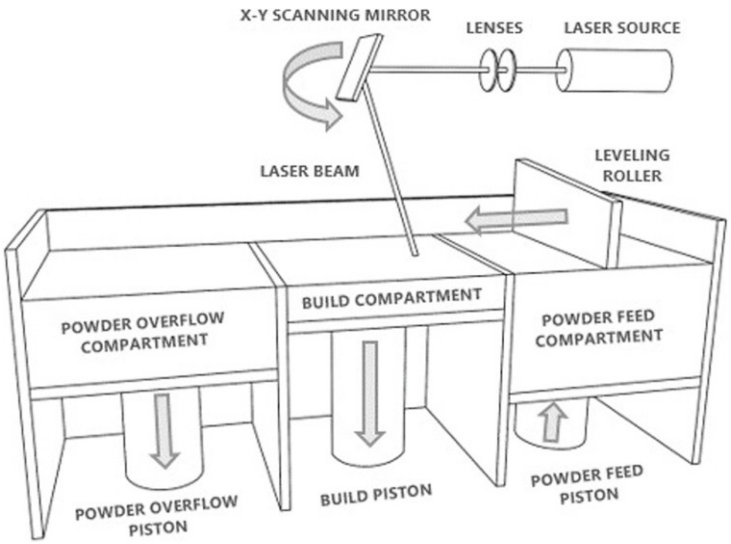

Figure 1: Schematic diagram of a DMLS system

A DMLS machine is composed by a process chamber with recoating system, elevating system and platform heating module, an optical system with an Yb (Ytterbium) fibre laser (400W), a process gas management system, a process computer with process control software.

The build chamber (Fig. 2), the zone where the part is physically created, layer after layer, can be divided into three main zones:

1. on the right, there is the "powder feed platform or dispenser": virgin or reused (and sieved) powder is put inside the tank and then compacted manually;
2. a recoater blade moves horizontally taking the powder from the dispenser and spreading it over the build platform. Here, the laser will physically build the component, layer after

layer;

3. on the left , the moving blade let the exceeding and unused powder drop into the powder overflow container.

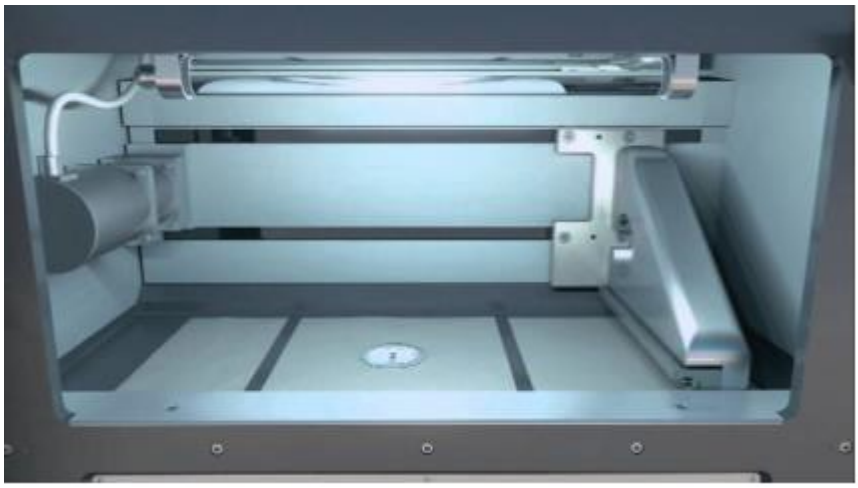

Figure 2: The build chamber of an EOS M280 printer

On the left, in blue, the powder overflow platform. In the middle, in red, the building platform. On the right, the powder feed platform (Fig.3).

Under the three platforms, pistons provide the right position of the different zones. This mechanical part of the machine is responsible of the perfect position of the working zone and of the precise thickness of the single layer, usually from 20 to 60 μm.

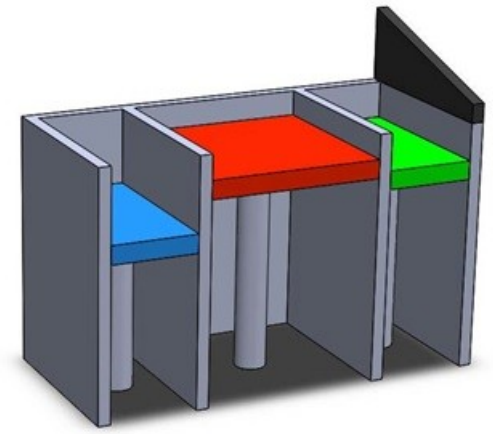

Figure 3: EOS M280 platform scheme.

2.1 PRINTING PROCESS

For the manufacture of any part, the machine performs the following steps. The building and the dispenser platforms are lowered by an amount equal to the thickness of a layer, so that the recoater blade can move without collision. When the recoater stands in right position, the dispenser platform rises to supply the amount of powder for a layer. Then the recoater moves from leftward and the metal powder is spread on the building platform. The exceeding powder falls into the collector. The scan head moves the laser beam through a two-dimensional cross section and the energy of the laser beam melts the powder in the exposed area, creating a metallic bond in the surrounding exposed material, including the previous layer. The recoater deposits another layer of powder as the building platform lowers and the dispenser one raises by the same amount again. This process proceeds layer-by-layer until all the parts in the so-called *printing job* are completed.

2.2 DATA PREPARATION

The AM equipment accept the geometric model in formats consisting of a mathematical representation of the geometry, so the CAD model must be converted. The most industrially relevant file format consists of an approximated representation of the solid as a sequence of planar triangular elements. This representation is called *STL* (*Standard Triangulation Language* or *Surface Tessellation Language*) and it is currently the industry standard to transfer the part data to the AM systems. An STL file is characterized by two widely used representations: ASCII and binary version. These formats represent each triangular facet by the coordinates of the three vertexes (ordered by the right-hand rule) and an outward normal represented by its vector (the direction of this vector differentiates internal and external surfaces of the part).

The tessellated representation involves several disadvantages. Problems are related to the triangulated boundary representation, because the curved surfaces can only be approximated by triangular facets: a large number of facets gives a high approximation accuracy, but it results in an extremely large amount of data. The maximum deviation between an original

surface of a CAD model and a triangle of the corresponding tessellated model is termed as *chordal error*. Due to the need of recreating the topology of the CAD model, proper data preparation is a prerequisite for the correct implementation of AM processes: poor data or data errors can result in poor parts quality, or even cause the failure of a job. This phase of the process is affected by countless geometric and topological parameters, some of which are listed in Table 1.

Table 1: Geometric and topological parameters

GEOMETRIC/TOPOLOGICAL PARAMETERS	AFFECTED CHARACTERISTICS
PART INCLINATION (BUILD ANGLE)	• Mechanical properties • Part accuracy • Process speed
PART POSITIONING ON THE PLATE	• Mechanical properties • Part accuracy • Shrinkage/distortion
PART ORIENTATION	• Mechanical properties • Part accuracy • Shrinkage/distortion
TYPE AND NUMBER OF SUPPORT	• Mechanical properties • Process speed • Wasted material amount • Surface roughness
Z-HEIGHT	• Process speed • Part accuracy • Surface roughness
LAYER THICKNESS	• Mechanical properties • Part accuracy • Process speed

In the DMLS process, as well as in most AM processes, supports are meant to prop up cantilever areas of components (Fig. 4). Once the job has been completed, they will be removed from the part. They represent the real waste of an ALM process: they do not belong to the printed part and cannot be reused in other 3D processes. A new challenge is therefore represented by the design and the conception of the part itself: the aim is to reduce the number of supports in order to reduce wastes. At the same time, machining will be required only where strict tolerances will be physically needed.

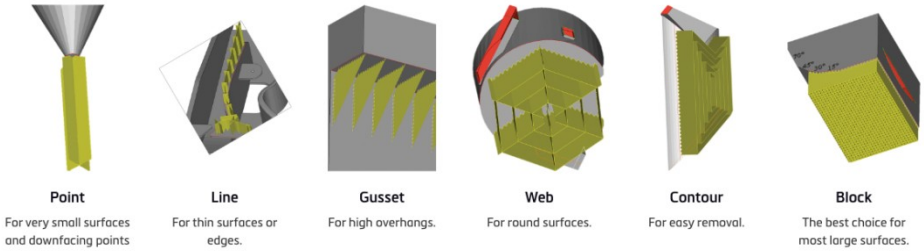

Figure 4: Several types of available supports

2.3 PRE-PRINTING PHASE

Before starting the printing process, it is necessary to setup and prepare the machine, by flooding both the machine itself and the re-circulating filter system with the appropriate inert gas, aimed to avoid material oxidation.

The printing phase is affected by a very large number of parameters. Tables 2 and 3 summarize the effects of the raw material properties and the ambient conditions on DMLS process, respectively.

Table 2: Effects of the raw material properties on DMLS process

MATERIAL PROPERTY	EFFECTS ON DMLS PROCESS
Particle Size Distribution (PSD)	Meltability Packing efficiency Surface roughness
Particle shape	Packing efficiency
Apparent/Tap density	Packing efficiency
Melting point	Indicator of energy requirements
Strength of green part	Facilitates part handling before thermal cycle (de-binding, sintering, infiltration)
Specific heat thermal conductivity	Heat transfer in powder bed
Void fraction	Residual porosity in printed parts
Flowability	Uniform spreading of powder layer

Table 3: Effects of the ambient conditions on DMLS process

AMBIENT CONDITIONS	AFFECTED CHARACTERISTIC
Room temperature too high	• Overload of the cooling system • Inadequate cooling of the optical assemblies • Formation of condensed water on cooled assemblies
Room temperature too low	Formation of condensed water on trim panels and housings
Ambient moisture content too high	Formation of condensed water on trim panels and housings
Inadequate supply of inert gas	Building process is interrupted

For the same raw material, the chemical and physical properties of the individual powder batch loaded into the printer affect the working conditions, the energy input, the part throughput and the post-processing. Anomalous values of these properties could generate variability within melting operations, hence in the final characteristics of the printed part.

If the powder storage conditions are not compliant to the specified requirements, the powder properties, and thus the AM process, may be negatively affected. For example, if the environment where the powder barrels are stored is too cold or too moist, or if the barrels are not properly sealed, the ambient moisture can condense within the metal powder, with the following results:

- *unevenness of the powder bed*: during the powder spreading, the metal particles adhere to each other, and to the recoater, thus resulting in poor quality of the powder bed;
- *pores formation within the part*: during the laser exposure, moisture in the metal powder can evaporate, generating pores within the sintered material, which drastically affect the part performance;
- *higher inert gas consumption*: during the laser exposure, water from the damp metal powder splits into oxygen and hydrogen, increasing the oxygen content in the process chamber and thus the consumption of inert gas.

The suppliers provide a specific datasheet for each kind of powder, containing material technical characteristics and specified conditions for storing. Each batch of powder is delivered together with a specific Certified Mill Test Report, CMTR.

2.4 POST-PROCESSING

Once a part has been completed and removed from the DMLS machine, the following post-processing steps are recommended:

- visual inspection;
- thermal treatment, for residual stresses relieving;
- support cutting, for the removal of the growth plate;
- growth support removal;
- finishing operations (tumbling, shot-peening/sandblasting or CNC machining).

The visual inspection allows the operator to verify that there is no evidence that the printing process has produced deformed, or not conforming to the expected size, parts(i.e. process compromised by lack of printing material).

Depending on the material and the intended application, the part may be then heat treated to relieve internal residual stresses and/or to get the desired mechanical properties.

Since the additively manufactured parts come out of the machine fused to the build platform, they must be separated. Two methods are commonly used: wire-electro- discharge machining (wire-EDM) and band saw. In addition, all the remaining support structures must be removed.

Shot-peening improves the part surface finish, changes the part colour to be slightly lighter and induces compressive surface stresses. According to the required surface quality, a more complex processing could be needed, such as CNC machining.

After removing the parts, the build platform must be resurfaced, by grinding or milling, to remove all the scraps of the support structures and to use it again.

CHAPTER 3 - STATISTICAL APPROACH FOR INDUSTRIAL EXPERIMENTS

3.1 OBJECTIVES OF AN EXPERIMENTATION

Additive Manufacturing is a complex, and rather new, technology that involves a large number of factors, related to both processing and post-processing parameters, to be investigated. Since most of its essential characteristics and outcomes can be only determined experimentally, the knowledge improvement of machine and process design, as well as the advancements in the processed materials, can be achieved through a series of experimental studies.

Classical and widespread One-Factor-At-a-Time (OFAT) experiments, that vary only one control factor, or variable, at a time while keeping the others fixed, can be not suitable for complex processes, because, as the number of factors to be studied increases, many test runs will be required, thus reflecting in much more time and money to be dedicated to the experimentation.

In order to design a new process, as well as to improve an existing one, a far more effective method is a computer-enhanced and systematic approach, that considers the impact of two or more factors on a response simultaneously. This approach is called *Design Of Experiments* (*DOE*) and corporations all around the world are adopting it as a cost-effective way to solve serious problems affecting their operations [14]. Besides the need of less resources for the same amount of information obtained, a designed experiment, unlike an OFAT one, allows the interaction between two, or more, control factors to be estimated systematically and the estimates of the effects of each factor are more precise. DOE also shows how interconnected factors respond over a wider region of the factor space, without the need to directly test all the possible values.

Any process can be seen as a combination of machines, methods and people, transforming some input into an output that can be characterized by one or more observable responses. In the scheme shown in Figure 5, x_1, x_2, …, x_n are the n input variables; y_1, y_2, …, y_m are the m possible system outputs selected for the analysis; z_1, z_2, …, z_p are the p uncontrollable variables, often referred to as noise. The factors can be quantitative or qualitative, but they should be both controllable. The system, or

theprocess, is viewed solely in terms of its input, output and transfer characteristics, without any knowledge of its internal working, so designed as a black box.

The objectives of the experiment may include the following:

- determining which variables are most influential on the response y;
- determining how to set the influential x so that y is almost always near the desired nominal value;
- determining how to set the influential *x* so that variability in y is very small;
- determining how to set the influential *x* so that the effects of the uncontrollable variables z_1, z_2, …, z_p are minimized.

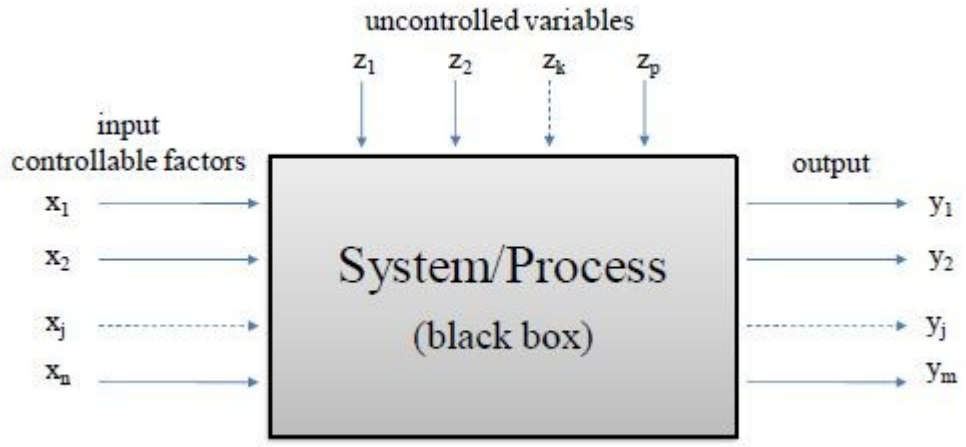

Figure 5: General model of a system or process

Furthermore, especially when a complex process is under investigation, a certain number of researchers or technicians, with distinct competences, are supposed to cooperate and statistical methodologies can help to catalyze the know-how in the process improvement, allowing a full and mature sharing of abilities and experience. In order to improve teamwork and to standardize information and experimental procedures within an interdisciplinary and/or international environment, it can result very useful to collect all helpful data, extracted from literature review or internal database, in a unique document, the *pre-design guide sheets*.

The Design Of Experiments represents an important tool to improve the performance of manufacturing processes. In many cases, it is the best way to establish which variables are important and the conditions under which these variables should work to optimize the process. It is also the only tool to perform efficient analysis of processes characterized by numerous parameters: all the factors are varied together and this represents the only way to discover interactions between the variables. The application of experimental design techniques early in the process development can result in improved process yields, reduced variability and closer conformance to nominal or target requirements, minimized development time and saved overall cost.

There are four main engineering problem areas in which DOE may be applied:

1. comparative, in which the engineer is interested in assessing whether a change in a single factor has in fact resulted in a change/improvement to the process;
2. screening/characterization, in which the engineer is interested in understanding the process, drawing out, after design and analysis, a ranked list of effective and ineffective factors involved in the process;
3. modelling, in which the engineer is interested in functionally modeling the process with the output being a good-fitting (high predictive power) mathematical function, and in having reliable (maximal accuracy) estimates of the coefficients in that function;
4. optimizing, in which the engineer is interested in determining optimal settings of the process factors, that is to determine for each factor the level that optimizes the process response.

The fundamental principles in planning experiments are [15]:

5. *randomization;*
6. *replicating;*
7. *blocking;*
8. *orthogonality;*
9. *factorial experimentation.*

Randomization is a method that protects against an unknown bias distorting the results of the experiment. An example of a bias is represented by the instrument drift in an experiment comparing a baseline procedure to a new procedure. If all tests are conducted first using the baseline procedure and then the new one, the observed difference between the procedures might be entirely due to instrument drift. To guard against erroneous conclusions, the testing sequence of the baseline (B) and new (N) procedures should be in random order such as B, N, N, B, N, B, and so on. In this way, the instrument drift or any unknown bias should average out.

Replicating augments the sample size and is a method for increasing the precision of the experiment. Replicating is essential to estimate the *experimental error*. A *replicate* is a complete repetition experimental run performed in the same experimental conditions, beginning with the initial setup: two, or more, measurements should be taken from each experimental unit at each combination of the experimental conditions. In addition, it is desirable to have some measurements taken at a later time, in order to test for repeatability over time. The first method (related to experimental condition *replicates*) gives an estimate of pure error, that is the ability of the experimental units to provide similar results under identical experimental conditions. Conversely, the second method (related to *repeated measurements*) provides an estimate of how closely the devices can reproduce measurements over time.

Blocking is a method for increasing precision by removing the effect of known nuisance factors. An example of a known nuisance factor is the batch-to-batch variability. In a blocked design, both the baseline and new procedures are applied to the samples of material from one batch, then to the samples from another batch, and so on. In this way, it is possible to detect if the difference between the new and the baseline procedures is affected by any batch-to-batch difference. Blocking is a restriction of complete randomization, since both procedures are always applied to each batch. Blocking increases precision since the batch-to-batch variability is removed from the "experimental error."

Orthogonality in an experiment results in the factor effects being uncorrelated and therefore more easily interpreted. The factors in an orthogonal experiment design are

varied independently of each other. The main results of data collected using this design can often be summarized by taking differences of averages and can be shown graphically by using simple plots of suitably chosen sets of averages. In these days of powerful computers and software, orthogonality is no longer a binding requirement, but it still results a desirable property because of the ease of explaining results.

Factorial experimentation is a method in which the effects due to each factor, as well as to their combinations, are estimated. Factorial designs are geometrically constructed and all the factors are varied simultaneously and orthogonally.

To improve the use of this technique, it is necessary to find the means of bringing together statistical concepts and practical knowledge in technical areas, such as material science or mechanical engineering. Moreover, it is necessary to create work-teams consisting of people with different skills, from knowledge of the involved tools and processes to advanced experience in the field of experimentation, and that all team members have a clear idea of the aim of the experiment. They must know the factors to be studied and how the experiment should be performed. It is also good that the ideas remain clear and the knowledge exchange continues during all the time of design and execution.

In this regard, Coleman and Montgomery identify some clear steps that split the procedure in order to achieve a correct and appropriate experimental plan of evidence [16]. They also suggest creating and filling in an iterative guide sheet.

3.2 GUIDELINES FOR DESIGNING EXPERIMENTS AND PRE-DESIGN GUIDE SHEETS

In order to help the experimenters to plan all activities needed for a good testing, the following steps are suggested to be performed when designing an experiment:

1) Recognition of the problem
2) Choice of factors and levels
3) Selection of the response variable(s)
4) Choice of experimental design
5) Conduction of the experiment

6) Data analysis

7) Conclusions and recommendations

3.3 Pre-design phase

The pre-design is the pre-experimental planning phase, relating to everything preceding the definition and the execution of an experiment. It corresponds to steps 1-3, previously suggested.

The use of pre-design guide sheets is intended to encourage the discussion and resolution of generic technical issues needed before the experimental design is developed, facilitating the interaction between statistical and technological competences.

3.3.1 Recognition of the problem

Before the data collection begins, all the specific questions that the researcher plans to examine must be clearly identified. First of all, the objectives of the experiment should be shared by all the members involved in the experimentation.

The objectives can be supported by relevant background, including information from previous experiments, routinely collected observational data, physical laws and expert opinions. This information can be useful to establish a context for the experiment to clearly understand what new knowledge can be gained, to motivate discussion about the relevant domain knowledge and to uncover possible experimental regions of particular interest and others that should be avoided.

In addition, a researcher should identify the sources of variability in the experimental conditions. One of the main goals of a designed experiment is to partition the effects of the sources of variability into distinct components, in order to examine specific questions of interest.

Two basic concepts have to be clear to the researcher in defining the problem and the questions to be addressed:

- population;
- sample.

A *population* is a collective whole of items from which researchers gather data. Before collecting any data, it is important that researchers clearly define the population, including a description of the members. The designed experiment should designate the population for which the problem will be examined. The entire population for which the researcher wants to draw conclusions will be the focus of the experiment.

A *sample* is one of the many possible sub-sets of units that are selected from the population of interest. In many data collection studies, the population of interest is assumed to be much larger in size than the sample so, potentially, there is a very large (usually considered infinite) number of possible samples. The results from a sample are then used to draw valid inferences about the population.

A *random sample* is a sub-set of units that are randomly selected from a population. A random sample represents the general population, or the conditions that are selected for the experiment, because the population of interest is too large to be investigated for whole. The use of techniques such as random selection after stratification or blocking is often preferred.

3.3.2 Choice of the factors and levels

In order to maximize confidence in the final results, it is important to consider all the relevant variables before the final data collection plan is approved. Figure 6 is a Venn diagram that illustrates different categories of factors affecting response variables. In the process for planning a designed experiment, the team classifies the different variables and factors and may choose to reassign them from one group to another. Inconclusive outcomes are likely to result if this classification is not adequately defined.

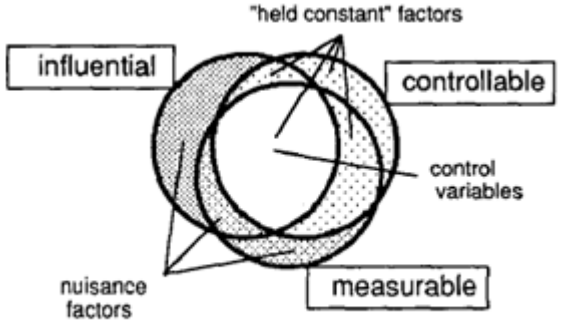

Figure 6: Different categories of factors affecting response variables

Control variables are independent variables that are possible sources of variation in the response. They are controllable and measurable and they can be attribute or continuous; in either case, they should be explicitly defined. These variables comprise the treatment and the design structures and are referred to as factors, or *primary factors*. Primary factors are controlled by the researcher and are expected to show the most interesting effects on the response variable(s). The most interesting levels should also be clearly defined for each primary factor.

The *levels* of the primary factors represent the range of inference space relative to the particular study. They can represent the entire range of possibilities of a random sub-set. It is also important to recognize and define when combinations of levels of two or more treatment factors are illogical or unlikely to exist.

Held-constant factors are controllable and measurable variables whose effects are not of interest in the experiment, so they are held constant over the duration of the study. This action increases the validity of the results by reducing extraneous sources of variation from entering the data. For this data collection plan, some of the variables that will be held constant include:

- the use of standard operating procedures;
- the use of one operator for each measuring device;
- all measurements taken at specific times and locations.

The standard operating procedure of a measuring device should be used in the most appropriate configuration and manner, according to both the developer and the technical user. Operator errors may affect results variability: to reduce this source of variation, one operator is often used for each measuring device, or specific training is given with the intent of achieving uniform results. *Nuisance factors* are variables that are known to exist, but the actual conditions prevent them from being manipulated, or it is very difficult to measure them because of cost or physical constraints. If a nuisance factor is not measurable and thought to be very influential, it may also be called an *experimental risk* factor. Such factors can inflate the experimental error, making more difficult to assess the significance of the control variables. The design of the experiment should eliminate or control these types of variables as much as possible in order to increase

confidence in the final results. Experiment designers have a set of passive strategies to reduce the impact of nuisance factors, such as randomization, blocking, analysis of covariance, stratified analysis.

3.3.3 Selection of the response variables

The aim of the DOE is *to assess the influence of primary factors, and their interactions, on the response of a generic process*.
The *response variables* represent the characteristics of the output that the researchers want to analyze and optimize.
A response variable:

- is preferably a continuous variable;
- should capture, as much as possible, a quantity, or quality, of interest for the experimental unit;
- should be in appropriate units;
- should be associated with a target, or desirable, condition (which motivates the experiment);
- is preferably obtained by non-destructive and non-damaging methods, so that repeated measures can be made and measurement error can be quantified;
- should not be near a natural boundary;
- preferably has constant variance over the range of experimentation.

3.3.4 Choice of the experimental design

After having chosen the control factors and their corresponding levels, on the basis of both the theoretical understanding of the problem parameters and the experience on similar problems, and selected the response variables that can provide adequate information about the process, the following step consists in defining the structure of the experimental design

to be implemented. It is important to take seriously into consideration the number of runs required for each design scheme, as well as the actual levels of each factor.

Drawing a design template is a good way to view the structure of the design factors: understanding the layout of the design through the visual representation of its primary factors results of great help to construct an appropriate statistical model [17].

Once the experimental design scheme has been settled, the array describing the parameters used in each run is produced.

Finally, it is worth remembering that DOE-based experiments are iterative. Since this methodology is based on the progressive acquisition of knowledge, it would be a mistake to schedule a single, large, exhaustive experiment.

3.3.5 Conduction of the experiment

When performing the experiment, according to the defined set of runs, it is important to monitor the process during all stages, as making mistakes in this stage could produce irrelevant output and actually frustrate the advantages offered by the experimental design method, in terms of the scientific validity of the experiment.

Before conducting the main experiment, performing some preliminary tests, or *trial runs*, is often useful. These tests provide information on the adequacy of the experimental material, a check on the measuring system, an overall idea of the experimental error and an opportunity to become familiar with the experimental techniques. This also provides a chance to review the decisions taken in the previous steps, if required.

Furthermore, it is important to precisely follow the data collection protocol when the data are collected. Prior to collecting the data, it is important to double-check that all the instruments are valid, reliable, and calibrated. After that is confirmed, it is worth taking time to explain the data collection procedures to the person who will be actually involved in collecting the data. It might seem counter-intuitive to technicians and machine operators to execute a randomized design. They might re-organize the data collection scheme in an effort to be more efficient, without realizing the impact that it might have on the experiment.

If the experiment is carried out successfully, the statistical analysis of the results can provide a solid way to determine the effects of all the control factors and their interactions on the response, as well as to detect if the results are affected by experimental errors.

3.4 CONCLUSIONS AND RECOMMENDATIONS

Once the data analysis has been completed, investigators should come to practical conclusions about the results and recommend a next course of action. In this phase, graphical methods for presenting and sharing the results are often useful. Furthermore, *control*, or *confirmation*, *tests* should be performed in order to validate the conclusions of the experiment.

CHAPTER 4 – MATERIALS AND FACILITIES

This work of thesis has been carried out using a 3D EOS M280 system (Fig. 7), based on DMLS technology, property of MBDA IT, located in Fusaro plant (Naples).
Experimental studies have been conducted in agreement with MBDA IT on alloys of its interest; in particular, an Aluminium alloy (AlSi10Mg), a Titanium alloy (Ti6Al4V) and two stainless steel (GP1 or 17-4 and PH1 or 15-5PH).
All powders come from EOS, who certifies both mechanical and chemical properties.

4.1 EOSINT M 280 system

Figure 7: EOSINT M 280 system

Basic information about each element are reported below:

- ✓ **EOSINT M 280**

Optical system:

- laser: Yb (Ytterbium) fibre laser, nominal power 400W, wavelength 1060÷1100 nm;
- scanner: exposure speed up to 7000 mm/s;
- focusing objective: focal length of F-theta (flat-field) lens 410 mm, diameter of laser beam at building area ≈100 μm;
- laser cooler: water-air cooler with 1.4 kW refrigerating capacity.

Building volume:

- including building platform: 250 mm x 250 mm x 325 mm.

Recoating system:

- stroke: ≥ 500 mm
- positioning speed: 40÷500 mm/s (typical ≈80 mm/s).

Elevating system:

- maximum height: 325 mm (incl. building platform);
- positioning speed: ≤ 5 mm/s;
- positioning repeatability: ≤ ± 0.005 mm;
- minimum layer thickness: 0.02 mm.

Thermal setting:

- sensor: temperature transducer Pt100 4;
- operating temperature: 35÷80°C, depending on metal powder.
-

- ✓ **Wet separator**

The wet separator is used to clean up metal powders and metal condensates. After being drawn up, the substances are separated in a water-filled container and the waste air is purified by a residual dust filter.

- ✓ **Elevator Trolley**

The elevator trolley is used to raise and transport building platforms, powder bins and other equipment. It can be set up with different lifting tackle items, depending on the specific tasks.

- ✓ **Conveying Module**

The conveying module is used for collecting and conveying the metal powder from the dispenser, building and collector ducts on the machine to a powder bin.
Suction time and emptying time can be adjusted to suit the type of metal powder used. The main and fine filters in the unit prevent particles of metal powder entering the waste air.

- ✓ **Sieving Module**

The sieving module is used to sieve, mix and homogenize the metal powder transported out of the machine. The used and unsieved powder is passed to the vibrating sieve via an inlet hose. The reusable material is separated from the oversized grains by ultrasonic vibration and collected into a powder bin.

- ✓ **Refill Module**

The refill module is used to enable a secure and user-friendly refilling of the feed compartment with the sieved metal powder.

4.2 AlSi10Mg

AlSi10Mg is a typical casting alloy with good casting properties and is typically used for cast parts with thin walls and complex geometry. It offers good strength, hardness and dynamic properties and is therefore also used for parts subject to high loads. Parts in EOS Aluminium AlSi10Mg are ideal for applications which require good thermal properties and low weight. Conventionally, printed parts with this aluminium alloy are often heat treated after the end of the job [18].

Table 4: Chemical compositional range of EOS Aluminium AlSi10Mg powders

Material composition	Al (balance) Si (9 ÷ 11 wt-%) Fe (≤ 0.55 wt-%) Cu (≤ 0.05 wt-%) Mn (≤ 0.45 wt-%) Mg (0.2 ÷ 0.45 wt-%) Ni (≤ 0.05 wt-%) Zn (≤ 0.10 wt-%) Pb (≤ 0.05 wt-%) Sn (≤ 0.05 wt-%) Ti (≤ 0.15 wt-%)

All AlSi10Mg specimens for the evaluation of mechanical properties were produced in Argon atmosphere, using the optimised sets of exposure parameters provided by the producer, the EOS Part Property Profiles *AlSi10Mg Speed 1.0 30µm* and heat treated at 300°C for 2 hours.

4.3 Ti6Al4V

Ti6AlV4 is well-known light alloy, characterized by having excellent mechanical properties and corrosion resistance combined with low specific weight. Ti64 material is ideal for many high-performance applications.

Parts built with EOS Titanium Ti64 powder can be machined, shot-peened and polished in as built and heat treated states. Due to the layer wise building method, the parts have a certain anisotropy [19].

Table 5: Chemical compositional range of EOS Titanium Ti6Al4V powders

Material composition	Ti (balance) Al (5.5 ÷ 6.75 wt-%) V (3.5 ÷ 4.5 wt-%) O (max 0.2 wt-%) N (max. 0.05 wt-%) H (max. 0.015 wt-%) Fe (max. 0.3 wt-%) Y (max. 0.015 wt-%) C (max. 0.08 wt-%)

All Ti6Al4V specimens for the evaluation of mechanical properties were produced in Argon atmosphere, using the optimised sets of exposure parameters provided by the producer, the EOS Part Property Profiles *Ti64_Performance 2.0 30 μm* and heat treated at 650°C for 2 hours.

4.4 PH1

Commonly used in medicine, aerospace and a variety of industrial applications where durability, solidity and corrosion resistance are required, EOS Stainless Steel. PH1 is a pre-alloyed stainless steel in fine powder form. Its composition corresponds to US classification 15-5 and European 1.4540. It has good corrosion resistance and excellent mechanical properties. This material is ideal for many part- building applications such as functional prototypes, small series products or spare parts [21].

Table 6: Chemical compositional range of EOS Stainless Steel PH1 powders

Material composition	Fe (balance) Cr (14 ÷ 15.5 wt-%) Ni (3.5 ÷ 5.5 wt-%) Cu (2.5 ÷ 4.5 wt-%) Mn (max. 1 wt-%) Si (max. 1 wt-%) Mo (max. 0.5 wt-%) Nb (0.15 ÷ 0.45 wt-%) C (max. 0.07 wt-%)

All the specimens for the evaluation of mechanical properties were produced in Nitrogen atmosphere, using the optimised sets of exposure parameters provided by the producer, the EOS Part Property Profiles *PH1_Surface 1.0 20 μm* and heat treated at 482°C for 4 hours.

4.5 GP1

Widely used in a variety of engineering applications, EOS Stainless Steel GP1 is a pre-alloyed stainless steel in fine powder form. Its composition corresponds to US classification 17-4 and European 1.4542. It is characterized by having good corrosion resistance and mechanical properties, especially excellent ductility in laser processed state. This material is ideal for many part-building applications such as functional metal prototypes, small series products or spare parts [20].

Table 7: Chemical compositional range of EOS Stainless Steel GP1 powders

Material composition	Fe (balance) Cr (15 ÷ 17.5 wt-%) Ni (3 ÷ 5 wt-%) Cu (3 ÷ 5 wt-%) Mn (max. 1 wt-%) Si (max. 1 wt-%) Mo (max. 0.5 wt-%) Nb (0.15 ÷ 0.45 wt-%) C (max. 0.07 wt-%)

Pre-alloyed 17-4 PH powder used in additive manufacturing can exhibit different microstructures depending on which gas is used for atomisation: the use of argon results in a martensitic powder, while that of nitrogen in an austenitic one.

The EOS GP1 powder is provided by the supplier as austenitic.

All the specimens for the evaluation of mechanical properties were printed in Nitrogen atmosphere, using the optimised sets of exposure parameters provided by the producer, the EOS Part Property Profiles *GP1_Surface 1.0 20 µm* and heat treated at 650°C for 1 hour.

CHAPTER 5 – RECYCLING METHODOLOGY

5.1 EXPERIMENTAL PROCEDURE

In order to identify the key aspects of previous investigations aimed to evaluate the possibility of reusing un-melted powder in PBF processes, an extended literature review was carried out. In [22], the effect of powder reuse on the mechanical properties of IN718 parts produced by SLM is assessed using a single 25 kg powder batch and considering an iterative procedure, in which all the powder is loaded into the SLM device for the fabrication of test samples; the produced samples are removed from the machine and stored apart for metallurgical and mechanical analysis; the residual powder is removed from the building chamber in order to be submitted to consecutive sieving and drying processes; part of the powder is collected for properties characterization; finally the sieved powder is loaded into the SLM device to start over the printing process again. Fourteen loops of this methodology are executed using an optimized set of exposure parameters for IN718. The effect of number of powder reuse for Inconel718 processed by SLM is examined again in [23], where a similar procedure is used also for Ti-6Al-4V powder. Other investigations on the aging process of Ti-6Al-4V powder material are carried out in [24] with a sixteen loops procedure on an industrial SLM equipment, in [25] with twenty-one loops on an EBM device and in [26], where the possibility of reusing powder up to thirty-eight times is assessed. In [27], a procedure to assess how many times a powder can be reused, based on the production of eight subsequent builds with a DMLS equipment with an initial 14-4 SS powder batch, is proposed. Even if they all refer to different AM technologies and different materials, the examined experimental procedures result to be quite similar: they all consist in an iterative printing procedure aimed to degrade metal powders. In this way, it should be possible to test if this degradation affects consistent characteristics of metal powders, as well as the physical and mechanical properties of the specimens produced at each iteration.

By combining the key features of all the analyzed approaches, *ten loops* of the following five-steps operative procedure, that could be representative of ordinary industrial practices, were executed.

As outlined in Fig. 8, a first DMLS build was produced using only virgin powder; at the

end of process, the build was removed from the machine and the unprocessed powder was collected, sieved and reloaded in the machine for the execution of the following DMLS run. This was iterated until the production of the last build. The samples produced within each build were used to evaluate the mechanical properties of the components, while powder samples were collected before starting each run to undergo chemical/physical analyses.

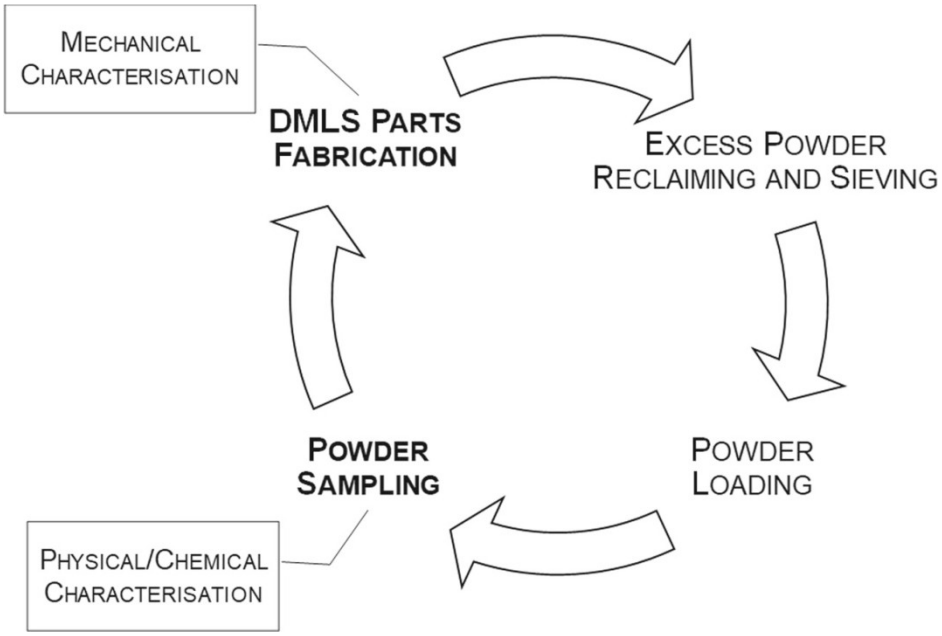

Figure 8: Operative procedure for powder reusing

Step by step, procedure for these tests are carried out as shown in Table 8.

Table 8: Printing procedures during recycled powder tests.

Step	*Description*	*Sampling*
Step 0	Beginning of Powder Recycling Test. A new Batch of powder is loaded into the printer	Powder sampling Moisture check
Step 1	EOS M280 starts printing the job	
Step 2	End of the job. All the powder inside the printer will be removed through IPCM (Conveying Module) module.	
Step 3	Removed powder is processed with the Sieving Module and stored in a sealed container containing air and a desiccant bag	
Step 4	The Building Plate is processed for support removal and rectified. Printer must be cleaned with the Vacuum Cleaner	
Step 5	The rectified Building Plate (or a new one) is placed in the printer along with the Sieved Powder	Powder sampling Moisture check
Step 6	Repeat Step 1 to Step 5 for nine (9) times	
Step 7	End of the Powder Recycling Test	

5.2 LAYOUT RECYCLING JOB

A single printed job contains:

- 6 six cylindrical bars to be used for Tensile tests
- 6 specimens to obtain High Cycle Fatigue specimens

This job (Fig. 9) has been printed 10 times, using the virgin or recycled powder according to the recycling strategy chosen for the specific alloy.

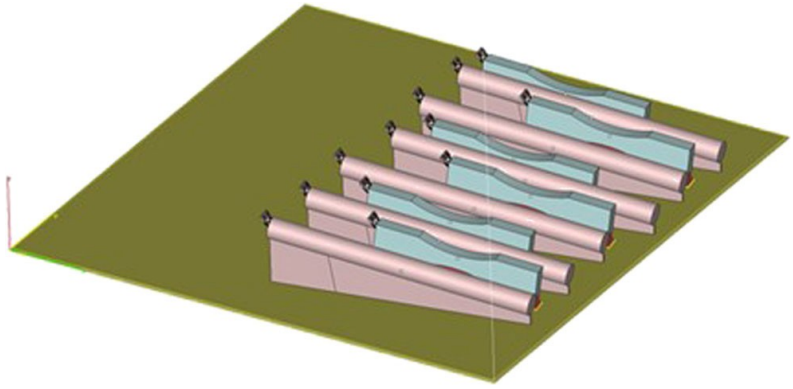

Figure 9: Specimens disposition on building platform

All the specimens were rotated by 13° with respect to the xy plane and by 10◦ with respect to the displacement direction of the re-coating blade to limit residual stresses and fluttering, respectively. In addition, they were all placed as rightmost as possible on the printing plate (at the beginning of the coater stroke) Fig. 10. Since the coater works better in this part, it ensures the best results in terms of part quality, while permitting to minimise the powder feedstock overdosing. The laser travel direction was rotated by 67° each layer.

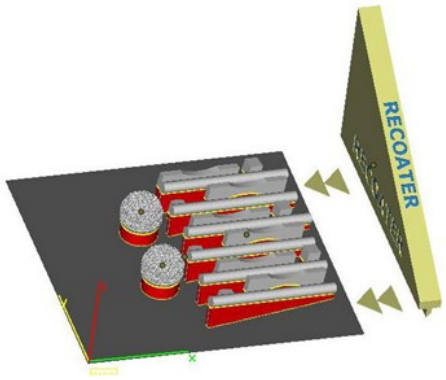

Figure 10: Specimens position on the building platform

5.3 RECYCLING STRATEGY

Two different strategies of recycling powder was followed:

5.3.1 Recycling Strategy 1

In AlSi10Mg jobs, content of *powder overflow container, building platform* and *powder feeding platform* have been brushed using a soft-bristled brush and collected using an aspirator. First, this powder amount is pre-filtered, in order to eliminate its moisture content. Then, it is passed through a sieve with 63 μm openings. At the end, the whole resulting mix of sieved powder has been used to fill the *charging zone* powder tank, previously empty.

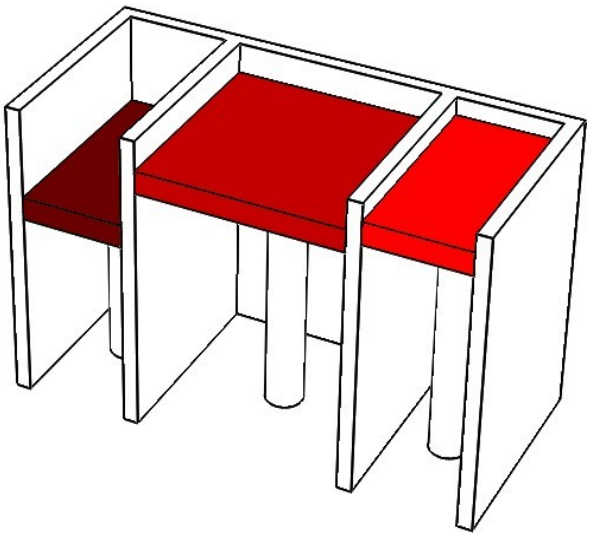

Figure 11: Recycling Strategy 1

5.3.2 Recycling Strategy 2

In stainless steel alloys GP1, PH1 and Ti6Al4V jobs, when the build is completed, content of both *powder overflow container* and *building platform* have been brushed using a soft-bristled brush and collected using an aspirator. First, this powder amount is pre-filtered, in order to eliminate its moisture content. Then, it is passed through a sieve with 63 μm openings. At the end, the whole resulting mix of sieved powder has been put *above* the virgin powder into the *feeding* powder container.

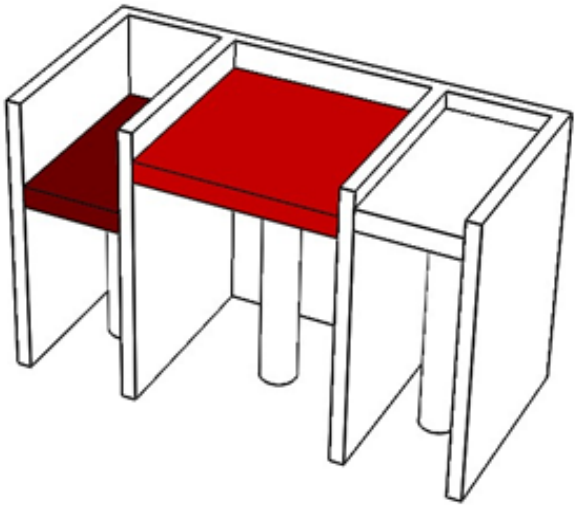

Figure 12: Recycling Strategy 2

Unlike recycling strategy 1, only the excess powder in the build volume and the overflow compartment was collected and sieved, and then loaded above the residual powder in the feeding compartment. This strategy have two industrial advantages:

- allows to save time and to simplify powder handling operations between two subsequent runs,
- does not imply to mix used powder with virgin one during the collecting phase.

For these reasons, this recycling strategy was used for the last three alloys to investigate.

5.4 SAMPLES AND TESTING STANDARD

Before starting each DMLS run, two powder samples were collected, in compliance with ASTM B215-15 [29], from the feeding compartment. The first one was instantaneously analysed to evaluate its moisture content, while the second was stored to later perform physical/chemical characterisation, as suggested in [30]. Particle size distribution (PSD) was determined according to ASTM B822-17 [31] using a Malvern MS2000 laser diffraction analyser, while particle morphology was evaluated using a Zeiss EVO/MA15 scanning electron microscope (SEM) according to ASTM F1877-16 [32].

Tap and apparent densities measurements were performed on a Mettler AJ 150 tester, in compliance with ISO 3953:2011 [33] and ISO 3923-1:2008 [34], respectively.

Finally, atomic emission plasma spectrometry (Thermo Fisher Scientific, model TJA Iris Advantage Radial) was used to measure powder elemental composition according to ASTM A751- 14a [35] and ASTM E1019-11 [36].

To evaluate the mechanical properties of parts additively manufactured with virgin and reused powder, forty DMLS builds (ten for each material) were produced. As shown in Fig. 9, each build hosted six cylindrical bars to be used for the tensile tests and six near net shape samples for the high cycle fatigue (HCF) test, afterwards machined to comply with ISO 6892-1:2016 [37] and DIN EN 6072:2011 [38], respectively, before undergoing mechanical testing. Tensile tests at room temperature were performed on an Instron 1185, with a crosshead speed of 0.45 mm/min, according to ASTM E8/E8M-16a [39].

HCF tests were performed, and terminated at 10^7 cycles, on a MTS Load Frame Model 312.21, with $K_t = 1$ and $R = 0.1$, according to ASTM E466-15 [40] to obtain the corresponding Wohler curves according to ASTM E739-10 [41].

CHAPTER 6 – EXPERIMENTAL RESULTS

Powder and printed specimens have been analysed in several ways and at different steps. First, a powder analysis was required to verify coherence between EOS Data Sheets and real chemical/physical characteristics. Then, a mechanical test campaign defined mechanical properties of the printed and machined specimens.

Powders analysis have been conducted to evaluate:

- Chemical composition
- Powder morphology
- Granulometric distribution
- Density (Tap/Apparent)

Mechanical analysis have been conducted to evaluate:

- Tensile properties
- High Cycle fatigue properties.

The one-way ANOVA was used to assess the effect of powder reuse times on the tensile properties of additively manufactured parts. The following response variables were considered:

- yield strength (YS 0.2%)
- ultimate tensile strength (UTS)
- elongation at break (A).

ANOVA techniques belong to the category of hypothesis tests. In particular, they are aimed to test the null hypothesis that the means of all populations are equal, against the alternative hypothesis that at least one is different. The effect of the control factor under investigation (in this case the *number of reuses* undergone by the powder) is considered statistically significant, as regards to the variability of the collected experimental observations, if the corresponding p value, calculated by the one-way ANOVA, is less than the set significance level, α.

The Minitab 19 software was used to perform the one-way ANOVA on the tensile test results at a confidence level of 95% (α = 0.05), after having removed any abnormal

observations and confirmed the assumptions of normal distribution and equal variance of the residuals.

HCF specimens was tested only for job 0, 4 and 9, for economic reasons.

In the following pages, all analysis and results are reported for each alloy separately.

6.1 AlSi10Mg

6.1.1 Powder analysis results

Chemical Analysis for AlSi10Mg powder are shown in Table 9 and plotted in Figure 13.

Table 9: AlSi10Mg chemical powders analysis

Results [%]										
	Job 0	**Job 1**	**Job 2**	**Job 3**	**Job 4**	**Job 5**	**Job 6**	**Job 7**	**Job 8**	**Job 9**
Cr	<0,01	<0,01	<0,01	<0,01	<0,01	<0,01	<0,01	<0,01	<0,01	<0,01
Al	Rest	Rest	Rest	Rest	Rest	Rest	Rest	Rest	Rest	Rest
Fe	0,20	0,21	0,21	0,23	0,22	0,21	0,21	0,21	0,20	0,20
Mn	0,01	0,02	0,02	0,02	0,02	0,02	0,01	0,02	0,02	0,02
Mg	0,43	0,45	0,44	0,45	0,43	0,45	0,45	0,45	0,45	0,43
Ni	<0,01	<0,01	<0,01	<0,01	<0,01	<0,01	<0,01	<0,01	<0,01	<0,01
Cu	<0,01	<0,01	<0,01	<0,01	<0,01	<0,01	<0,01	<0,01	<0,01	<0,01
Si	10,3	10,9	10,5	10,5	10,3	10,7	10,4	10,8	10,7	10,5
Zn	<0,03	<0,03	<0,03	<0,03	<0,03	<0,03	<0,03	<0,03	<0,03	<0,03
Pb	<0,01	<0,01	<0,01	<0,01	<0,01	<0,01	<0,01	<0,01	<0,01	<0,01
Sn	<0,01	<0,01	<0,01	<0,01	<0,01	<0,01	<0,01	<0,01	<0,01	<0,01
Ti	<0,01	<0,01	<0,01	<0,01	<0,01	<0,01	<0,01	<0,01	<0,01	<0,01
V	<0,01	<0,01	<0,01	<0,01	<0,01	<0,01	<0,01	<0,01	<0,01	<0,01
Zr	<0,01	<0,01	<0,01	<0,01	<0,01	<0,01	<0,01	<0,01	<0,01	<0,01

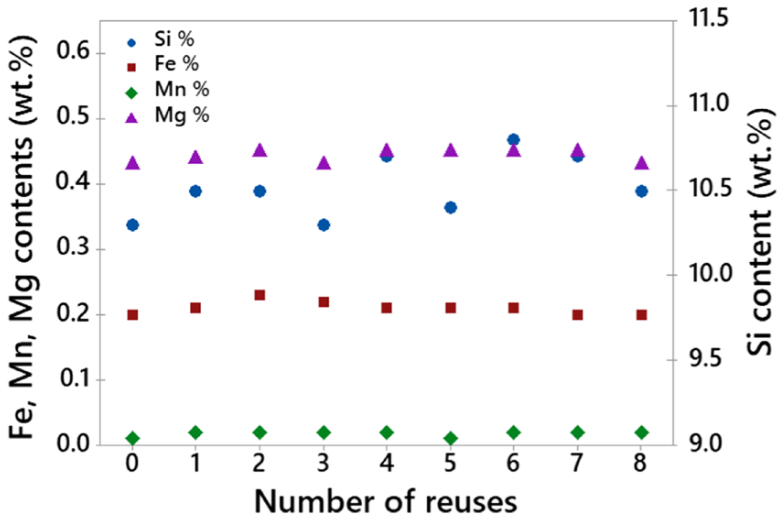

Figure 13: trends of iron, manganese, magnesium and silicon contents in the AlSi10Mg powder versus reuse times

The chemical composition of the reused powder remained almost constant during the whole experiment.

SEM images of AlSi10Mg powder particles are proposed. Please note that, in order to better appreciate a different shape of powder, first images refer to virgin powder. Second images are related to a four-times reused powder. Last ones, belong to a nine-times reused powder. This choice is directly linked to High Cycle Fatigue tests, were specimens number 0, 4 and 9 have been selected.

The shape of the AlSi10Mg particles is predominantly spherical over the nine runs (Fig. 14).

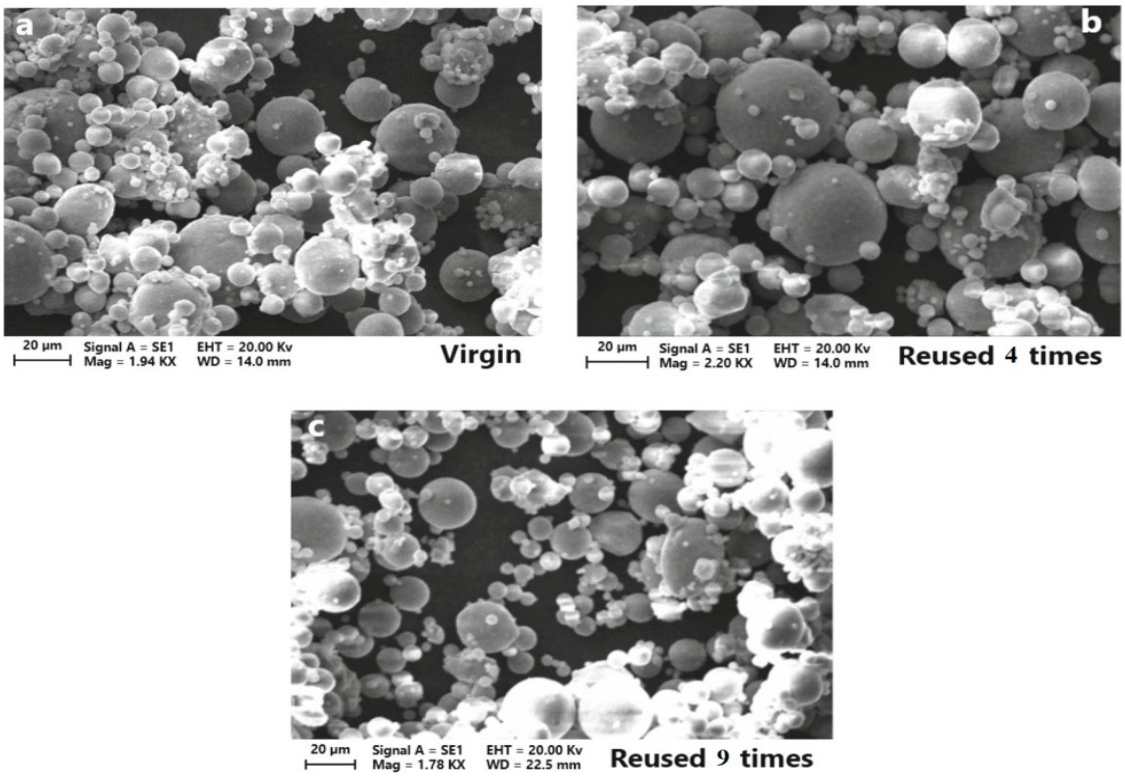

Figure 14: SEM images of the AlSi10Mg powder: a) virgin, b) reused four times, c) reused nine times

Granulometic distribution results for AlSi10Mg are expressed as average diameter of the particles at 10%, 50% and 90% of the cumulative volume distribution (i.e. D10, D50 and D90 percentiles) and presented in Table 10 and Figure 15b.

Table 10: Mean value, 10th (*D*10), 50th (*D*50) and 90th (*D*90) percentiles of the AlSi10Mg particle diameter

Results			
Number of reuses	***D10 [µm]***	***D50 [µm]***	***D90 [µm]***
0	12,4	31,6	58,5
1	10,9	29,1	55,2
2	10,7	28,3	53,9
3	10,7	28,1	53,5
4	10,3	27,3	52,5
5	10,2	26,8	51,6
6	10,1	26,8	51,6
7	9,88	26	51,2
8	9,96	26	50,7
9	9,74	25,8	50,4

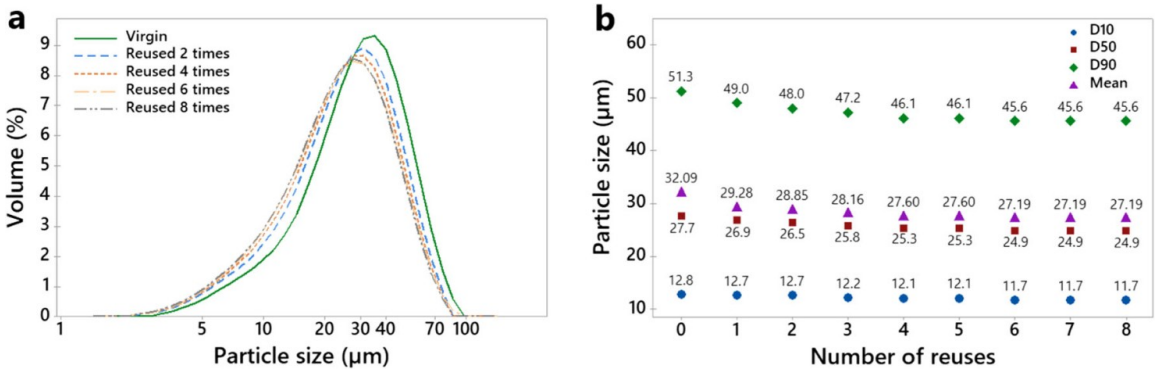

Figure 15: Particle size distribution of the AlSi10Mg powder versus reuse times. a) Probability density size distributions. b) Mean value, 10th (*D*10), 50th (*D*50) and 90th (*D*90) percentiles of the particle diameter

The particle size distributions (PSDs) of the reused powder exhibited a slight gradual leftward shift over the reuse times, pointing out a progressive reduction of larger particles content, as shown in Fig.15.

Table 11: Tap density and apparent density of the AlSi10Mg powder over number of reuses

Number of reuses	*Apparent Density [g/cm³]*	*Tap Density [g/cm³]*
0	1,08	1,36
1	1,06	1,4
2	1,13	1,46
3	1,1	1,45
4	1,13	1,42
5	1,15	1,45
6	1,18	1,46
7	1,17	1,49
8	1.16	1,48
9	1.14	1,50

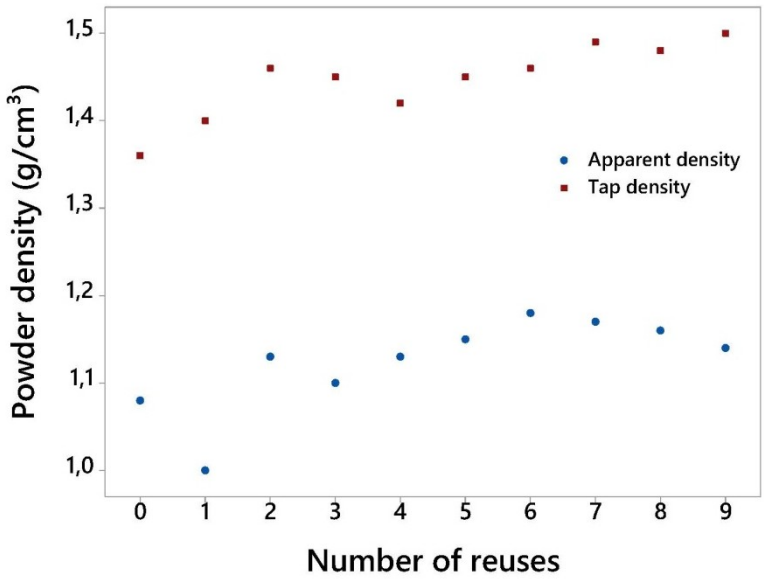

Figure 16: Tap density and apparent density of the AlSi10Mg powder over number of reuses

Chemical composition, tap density, apparent density and particle shape remained globally stable and compliant to the process requirements over reuse times.

6.1.2 Mechanical tests results:

The ANOVA results for the analysed tensile properties are reported in Table 12. The effect of powder reuse showed to significantly affect yield strength and ultimate tensile strength (p value = 0.000), with a progressive decrease of mechanical properties over the number of reuses, as shown in Table 12. Conversely, the observed variability in terms of elongation at break is shown to be purely physiological (p value >> 0.05).

The outcomes of the statistical analysis are confirmed by the slight variation in the shape of stress-strain curves over number of reuses. Figure 18 shows an example of stress-strain curves for the AlSi10Mg samples additively manufactured from virgin and reused powder, highlighting the slight decay of yield and ultimate strength over reuse times.

Stress-strain curves of the specimens produced within the same job were nearly superimposable, so only one for job was reported as reference.

With regard to the cyclic behaviour, Fig. 19 shows the Wohler curves of specimens produced with virgin and reused powder. Overall, the fatigue behaviour remained stable, even if with a slight decrease over reuse times, with a minimum high cycle fatigue strength ($\Delta\sigma$) of 145 MPa.

However, it is worth noting that the cyclic behaviour is inherently characterised by a certain uncertainty, since it depends on the presence of defects within the material.

Table 12: One-way ANOVA results for the AlSi10Mg tensile properties

Variable	Source	DOF	Adj SS	F-value	p value
YS 0.2%	Number of reuses	9	523.61	78.02	0.000
	Error	41	34.40		
	Total	49			
UTS	Number of reuses	9	691.12	138.91	0.000
	Error	41	25.50		
	Total	49			
A	Number of reuses	9	15.23	0.91	0.518
	Error	43	90.00		
	Total	51			

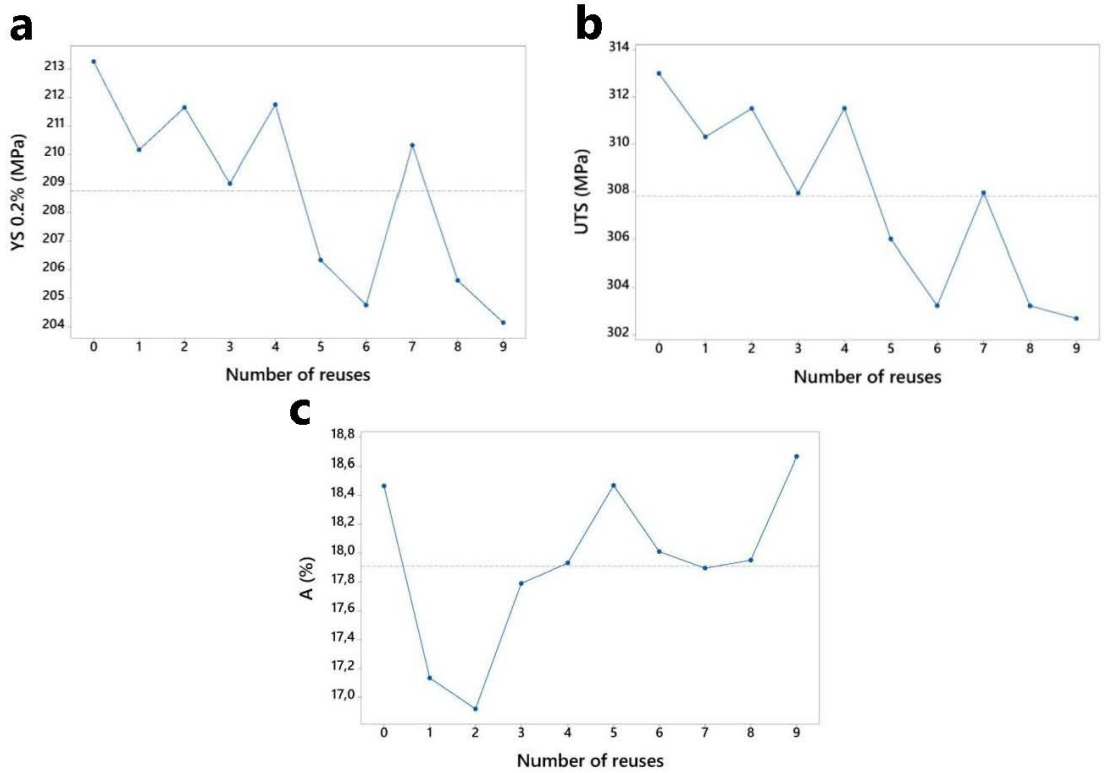

Figure 17: Main Effects Plots for the effect of number of reuses on AlSi10Mg tensile properties.

a) Yield strength. b) Ultimate tensile strength. c) Elongation at break

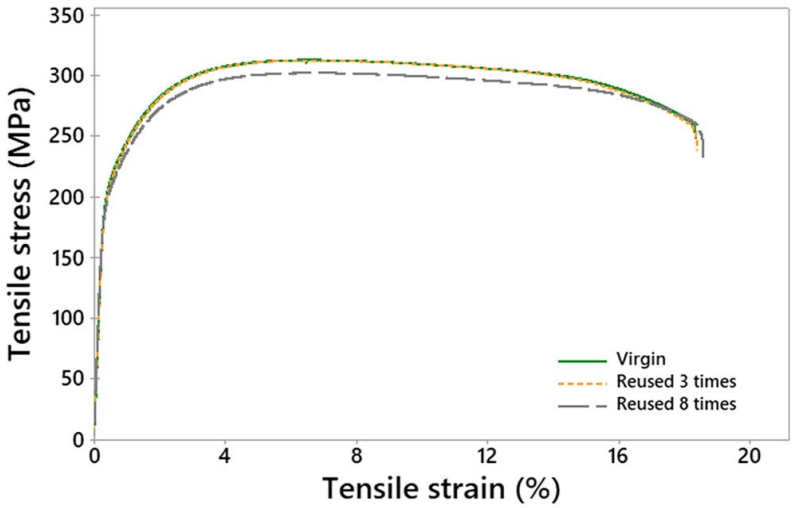

Figure 18: Stress-strain curves of AlSi10Mg specimens additively manufactured from virgin and reused powder

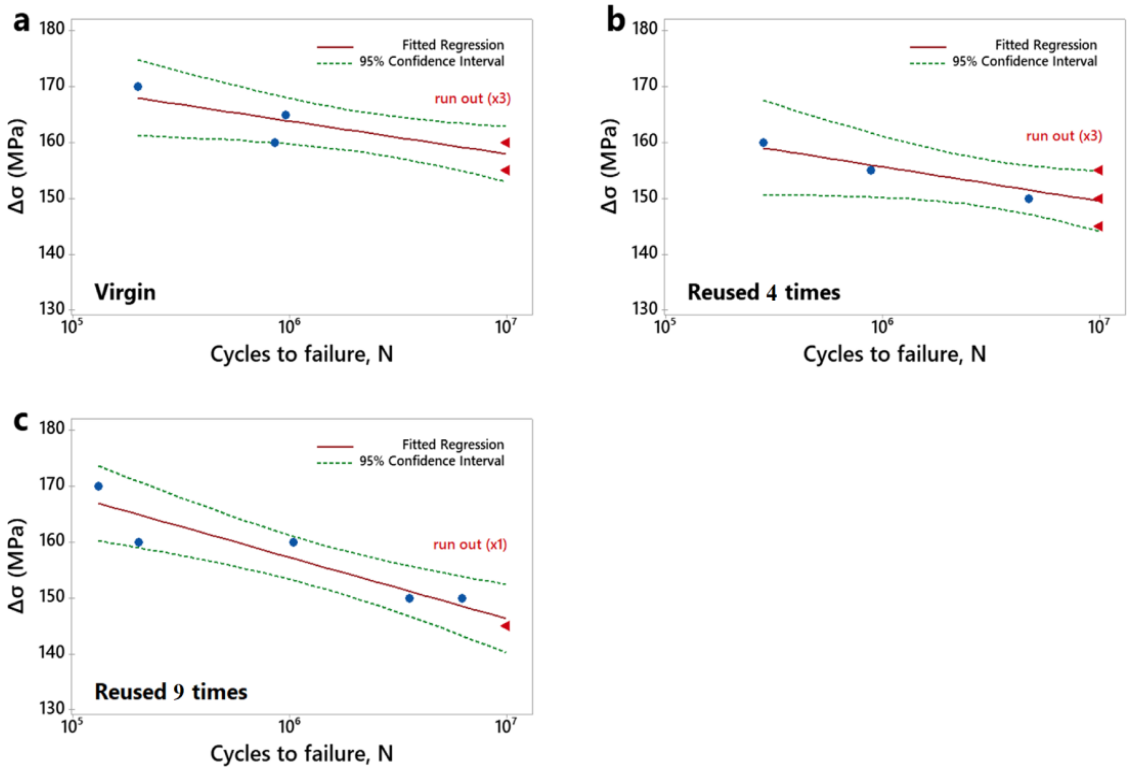

Figure 19: Wohler curves of the AlSi10Mg specimens additively manufactured from virgin and reused powder: a) virgin, b) reused four times and c) reused nine times

6.2 Ti6Al4V

6.2.1 Powder analysis results

Chemical Analysis for Ti6Al4V powder are shown in Table 13 and plotted in Figure 20.

Table 13: Ti6Al4V chemical powders analysis

Results [%]										
Chemical Analysis [%]	**Job 0**	**Job 1**	**Job 2**	**Job 3**	**Job 4**	**Job 5**	**Job 6**	**Job 7**	**Job 8**	**Job 9**
C	0,01	0,01	0,01	0,01	0,01	<0,01	/	0,02	0,01	0,01
Al	6,25	5,98	6,08	6,14	6,58	6,57	/	6,57	6,62	6,36
Fe	0,19	0,18	0,18	0,18	0,2	0,19	/	0,39	0,35	0,3
O	0,08	0,014	0,12	0,13	0,11	0,13	/	0,11	0,11	0,11
N	0,01	0,01	0,01	0,01	0,01	0,01	/	0,01	0,01	0,01
Ti	Rest	Rest	Rest	Rest	Rest	Rest	/	Rest	Rest	Rest
V	4	3,8	3,8	3,8	4,3	4	/	4	4	4
H	0,001	0,002	0.002	0,002	0,001	0,002	/	0,002	0,002	0,002

Please note that one powder specimen of Ti6Al4V alloy have been lost during tests (Job 6). Chemical results are therefore available for nine Ti6Al4V specimens families only.

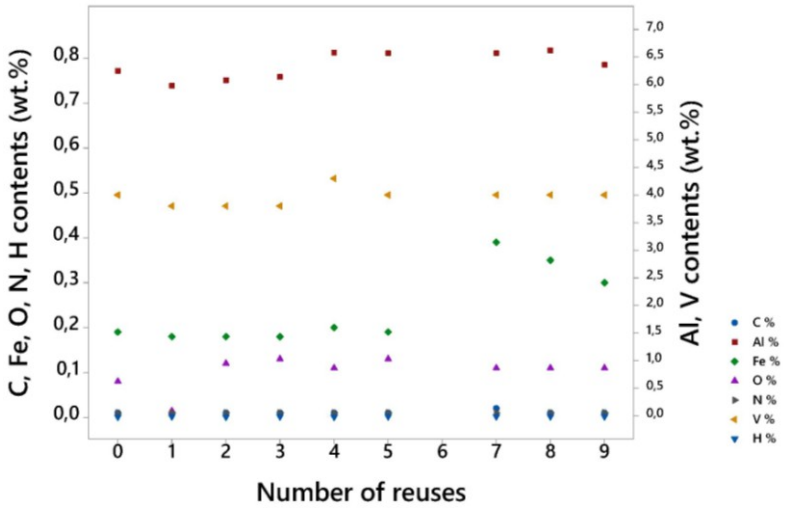

Figure 20: Chemical Ti6Al4V powder composition versus reuse times

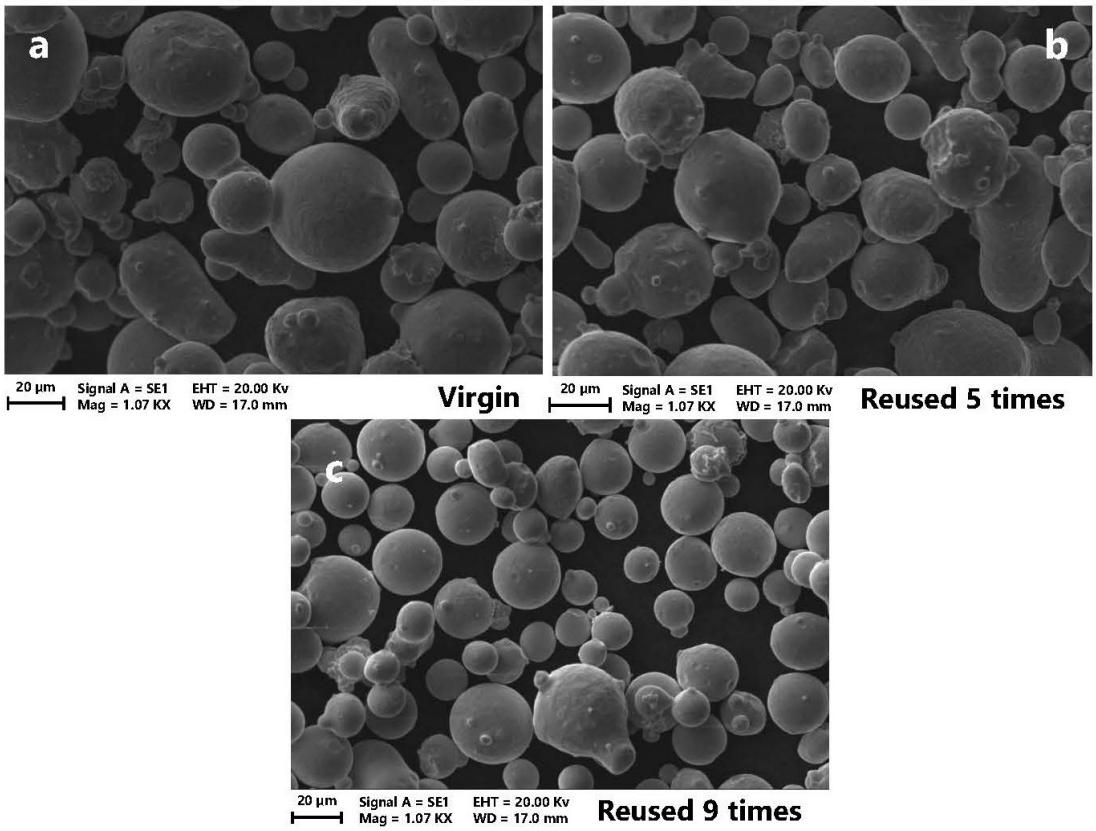

Figure 21: SEM images of the Ti6Al4V powder: a) virgin, b) reused four times, c) reused nine times

Granulometic distribution results for Ti6Al4V are expressed as average diameter of the particles at 10%, 50% and 90% of the cumulative volume distribution (i.e. D10, D50 and D90 percentiles) and presented in Table 14 and Figure 22.

Table 14: Mean value, 10th (*D*10), 50th (*D*50) and 90th (*D*90) percentiles of Ti6Al4V particle diameter

Results			
Number of reuses	***D10 [µm]***	***D50 [µm]***	***D90 [µm]***
0	24,9	38	57,1
1	25,4	38,4	57
2	25,3	38,3	57
3	25,1	38,1	56,8
4	24,4	36,9	55,3
5	23,6	37,8	58,8
6	/	/	/
7	25,5	38,6	57,7
8	26,4	39,9	59,8
9	25	38,3	48

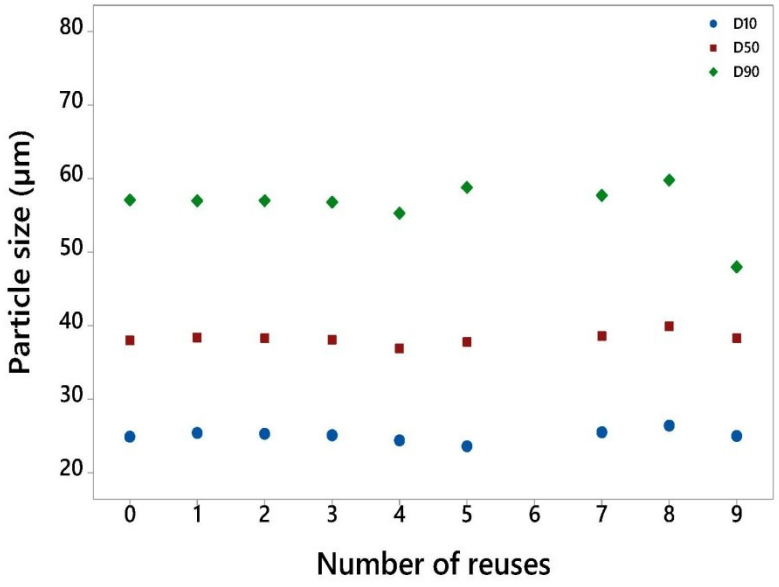

Figure 22: Mean value, 10th (*D*10), 50th (*D*50) and 90th (*D*90) percentiles of Ti6Al4V particle diameter

Table 15: Tap density and apparent density of the Ti6Al4V powder over number of reuses

Number of reuses	*Apparent Density [g/cm³]*	*Tap Density [g/cm³]*
0	2,3	2,7
1	2,4	2,7
2	2,4	2,7
3	2,4	2,7
4	2,4	2,7
5	2,4	2,7
6	/	/
7	2,4	2,7
8	2,4	2,7
9	2,4	2,7

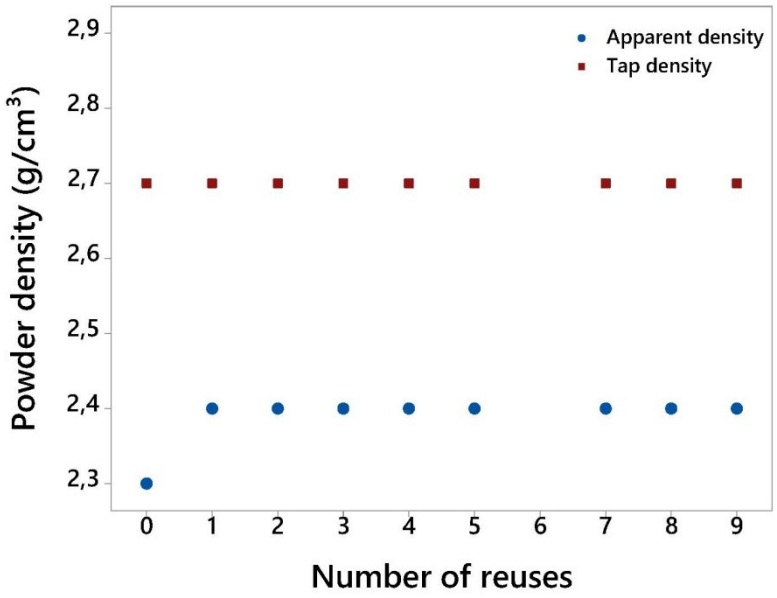

Figure 23: Tap density and apparent density of the Ti6Al4V powder over number of reuses

Chemical composition, tap density, apparent density and particle shape remained globally stable and compliant to the process requirements over reuse times.

6.2.2 Mechanical tests results

The ANOVA results for the analysed tensile properties are reported in Table 16. The effect of powder reuse showed to significantly affect yield strength and ultimate tensile strength (p value = 0.000), with a progressive increase of mechanical properties over the number of reuses, as shown in Table 16. Conversely, the observed variability in terms of elongation at break is shown to be purely physiological (p value >> 0.05).

The outcomes of the statistical analysis are confirmed by the slight variation in the shape of stress-strain curves over number of reuses (Fig. 25). With regard to the cyclic behaviour, Fig. 26 shows the Wohler curves of specimens produced with virgin and reused powder. Overall, the fatigue behaviour remained stable.

Table 16: One-way ANOVA results for the Ti6Al4V tensile properties

Variable	Source	DOF	Adj SS	F-value	p value
YS 0.2%	Number of reuses	9	17988	26.67	0.000
	Error	50	3747		
	Total	59			
UTS	Number of reuses	9	12874.6	85.17	0.000
	Error	50	839.8		
	Total	59			
A	Number of reuses	9	5.006	1.02	0.440
	Error	50	27.681		
	Total	59			

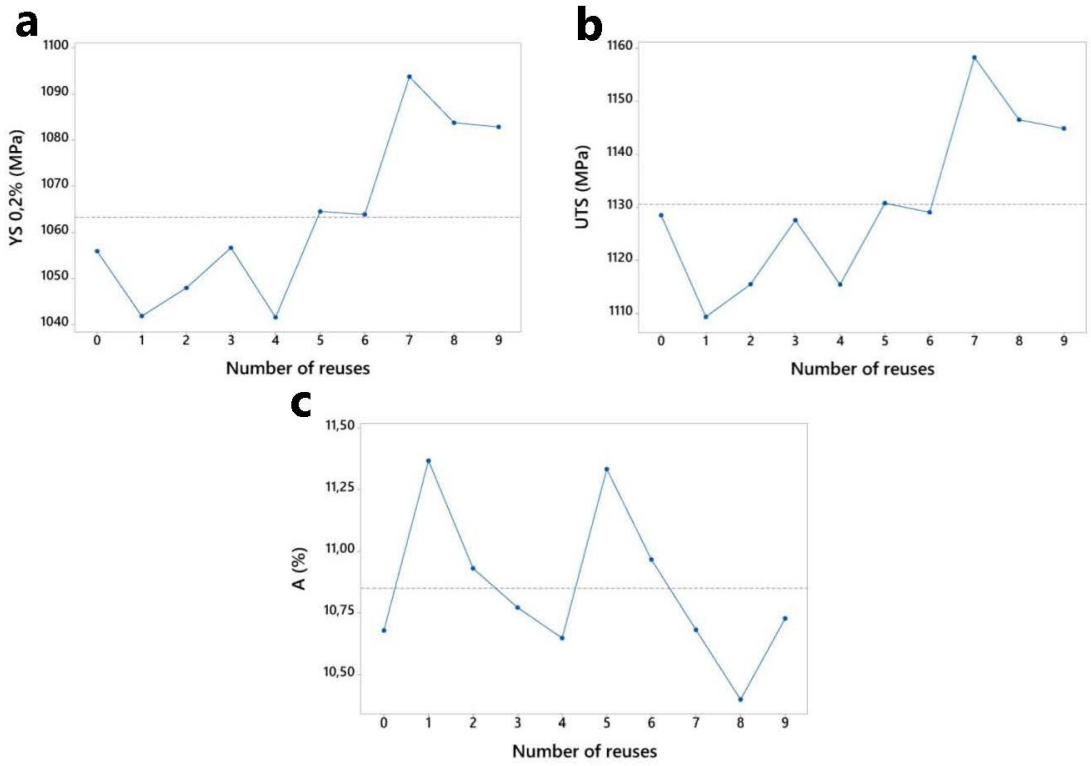

Figure 24: Main Effects Plots for the effect of number of reuses on Ti6Al4V tensile properties.

a) Yield strength. b) Ultimate tensile strength. c) Elongation at break

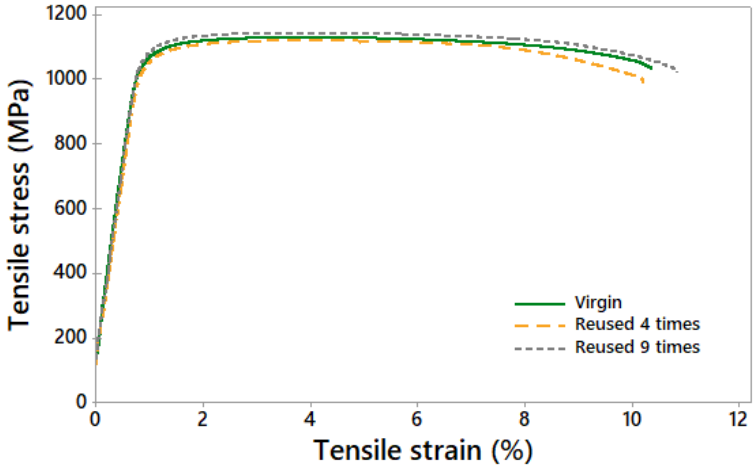

Figure 25: Stress-strain curves of Ti6Al4V specimens additively manufactured from virgin and reused powder

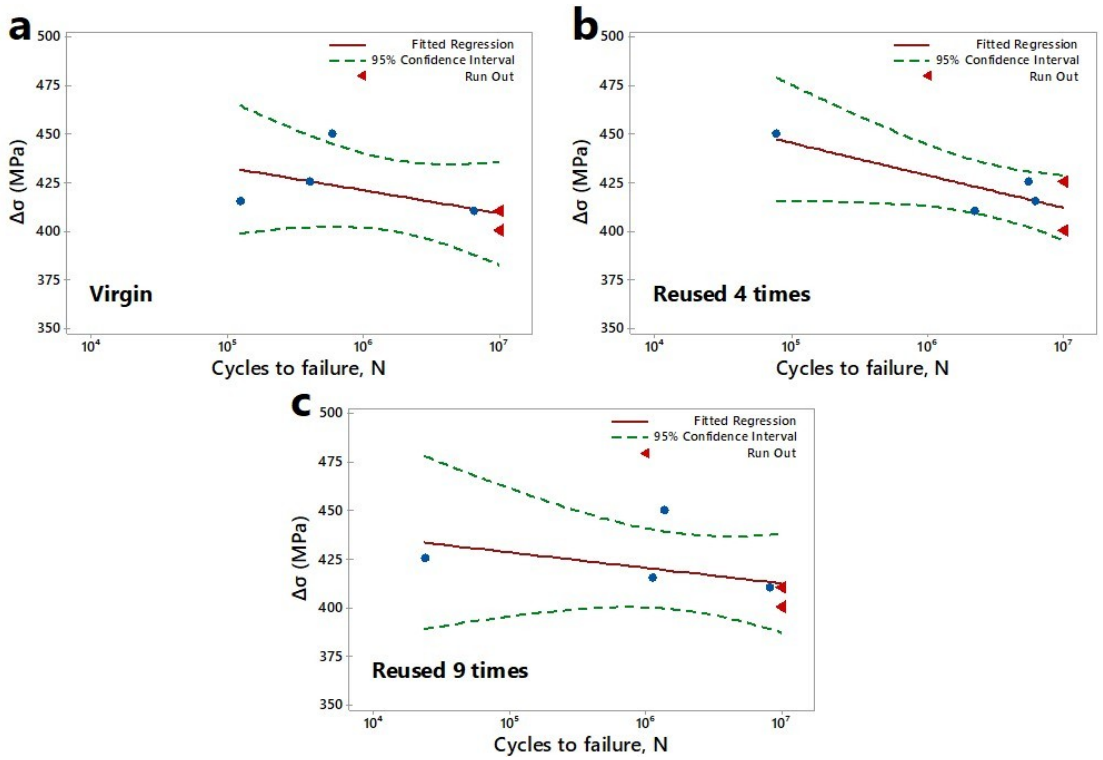

Figure 26: Wohler curves of the Ti6Al4V HCF samples produced with virgin and reused powder. a) Virgin. b) Reused 4 times. c) Reused 9 times

6.2.3 Technological investigation

The chemical composition of job 7, 8 and 9 show a significant increase in iron content, even if the percentage of iron is still acceptable for all the specimens because its values fall into the standards of ASTM B265-15, a metallographic and chemical investigation was carried out to assess the reason of this Fe increase.

The attention was focused on job 0, 4 and 8. The specimens have been polished with different degree of polishing papers, treated with diamond and alumina abrasive powders and etched using 5% hydrofluoric acid (HF) for about 40 sec. The microstructure has been studied both at the edge and the centre of specimens because after the etching treatment a visible ring has been observed on the specimens surface (Fig. 28).

Figure 27: Appearance of Job 0 after the etching process

In addition, the chemical composition analysis has been performed by EDX spectroscopy. Therefore, SEM images and chemical composition analysis at the edge and centre of Job 0 are reported in Figure 28, 29, 30 and 31 respectively.

Microstructure at the edge and centre of Job 0 are similar but the lamellar structures are less long at the centre of the specimen. Anyway, the chemical composition at the centre and edge of Job 0 is identical as confirmed by EDX analysis. The reason for this difference resides on low thermal conductivities in titanium alloys and thus, the centre cools more slowly than the edge after the heat treatment of the Ti6Al4V printed specimen.

Microstructure and chemical analysis at the edge and the center of Job 4 and 8 specimens are shown in Figures 32, 33, 34, 35, 36, 37, 38 and 39. As it is possible to note, both Job 4 and 8 have the same chemical and microstructural properties of Job 0.

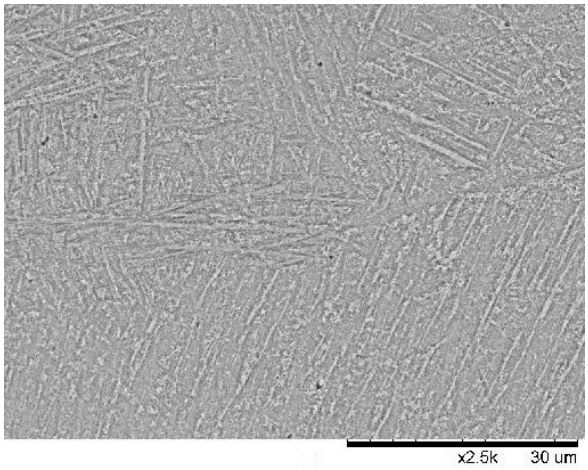

Figure 28: Ti6Al4V Job 0 microstructure at the edge of the specimen - SEM image.

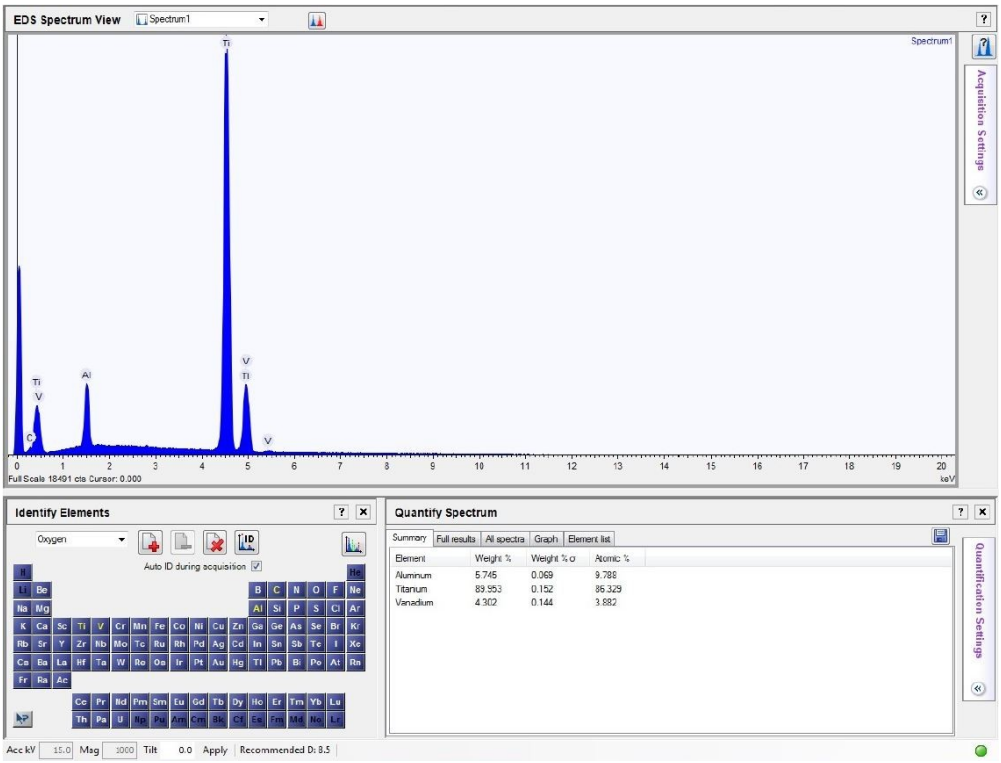

Figure 29: Ti6Al4V Job 0 chemical composition analysis at the edge of the specimen with EDX spectroscopy.

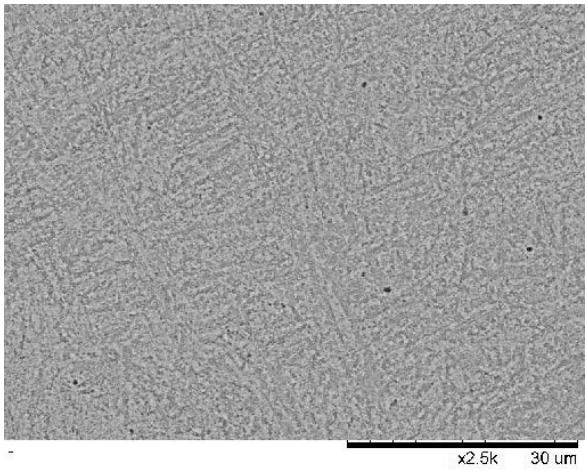

Figure 30: Ti6Al4V Job 0 microstructure at the center of the specimen - SEM image.

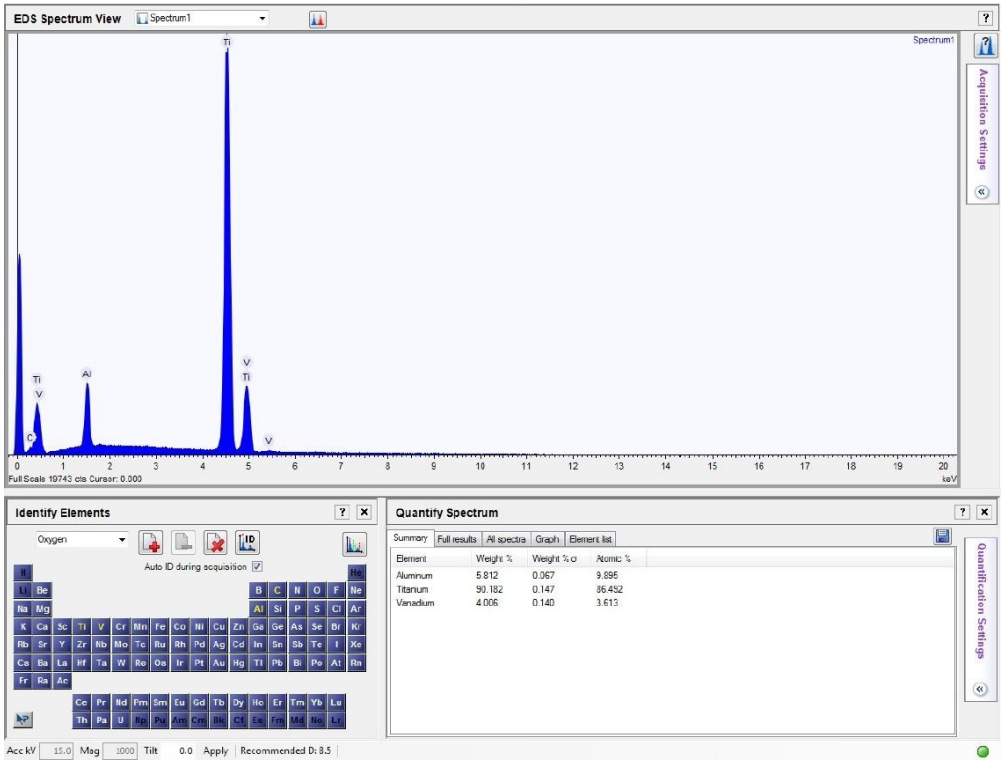

Figure 31: Ti6Al4V Job 0 chemical composition analysis at the ter of the specimen with EDX spectroscopy.

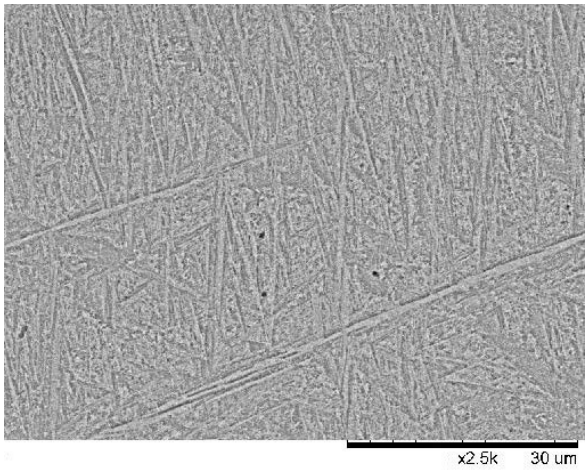

Figure 32: Ti6Al4V Job 4 microstructure at the edge of the specimen - SEM image.

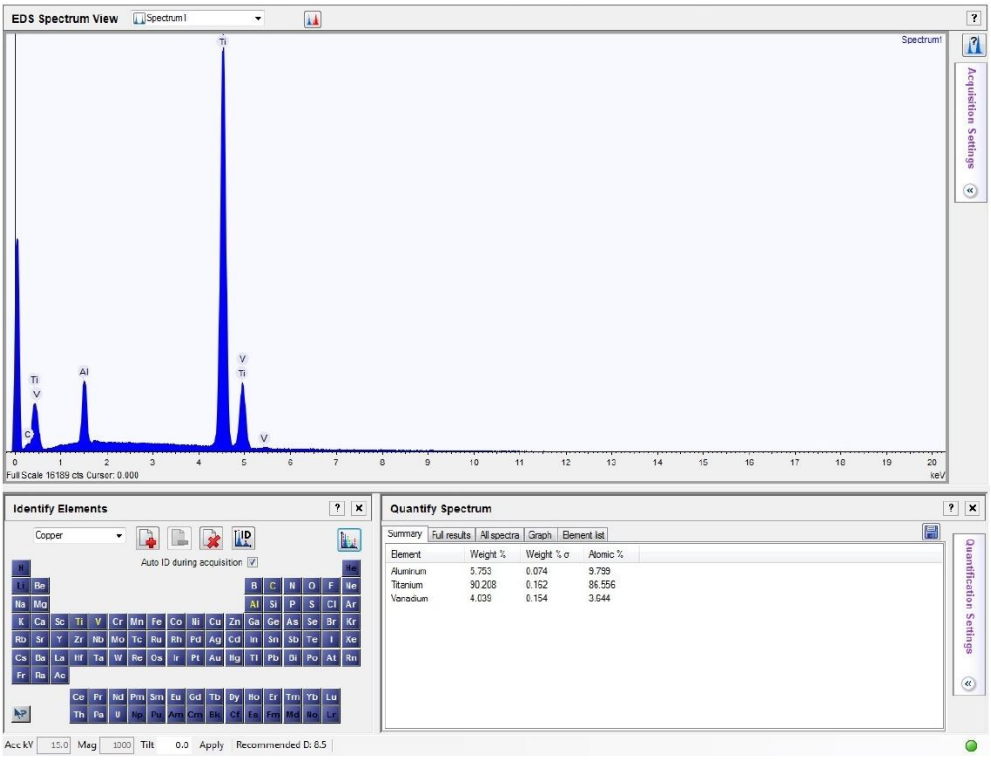

Figure 33: Ti6Al4V Job 4 chemical composition analysis at the edge of the specimen with EDX spectroscopy.

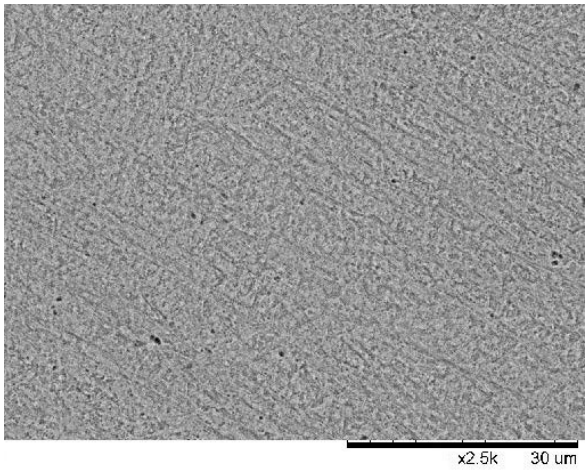

Figure 34: Ti6Al4V Job 4 microstructure at the center of the specimen - SEM image.

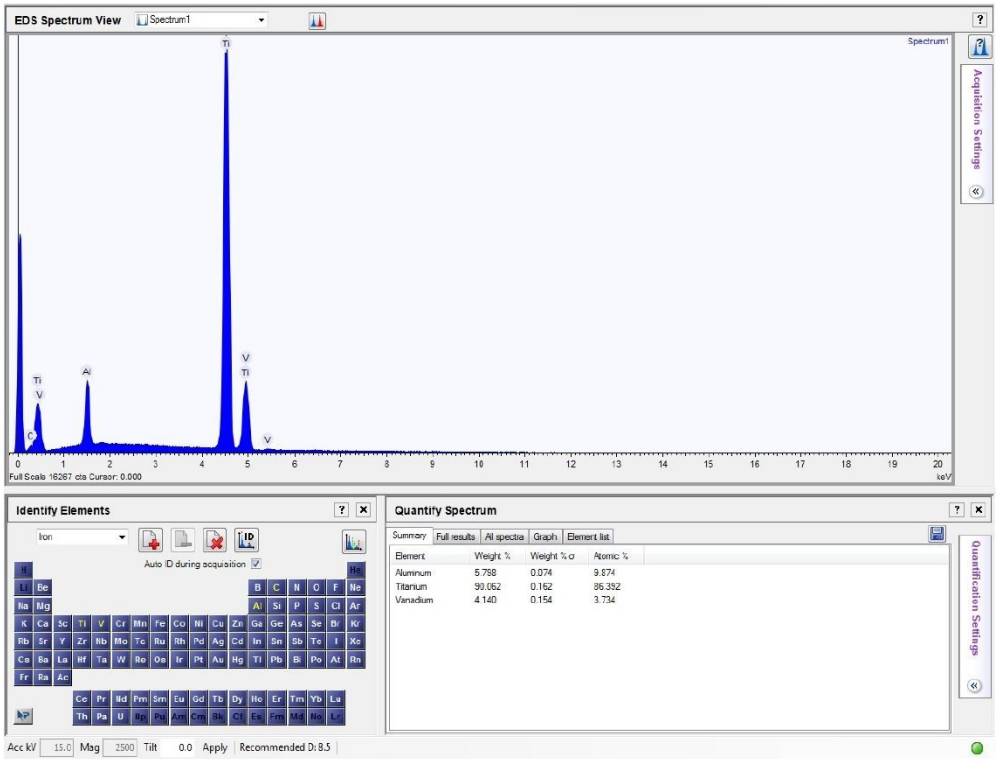

Figure 35: Ti6Al4V Job 4 chemical composition analysis at the center of the specimen with EDX spectroscopy.

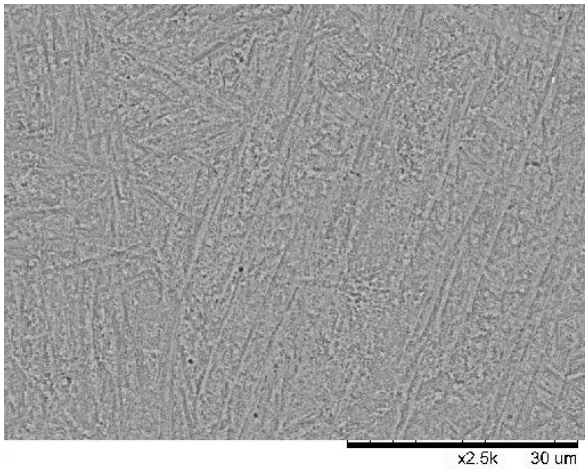

Figure 36: Ti6Al4V Job 8 microstructure at the edge of the specimen - SEM image.

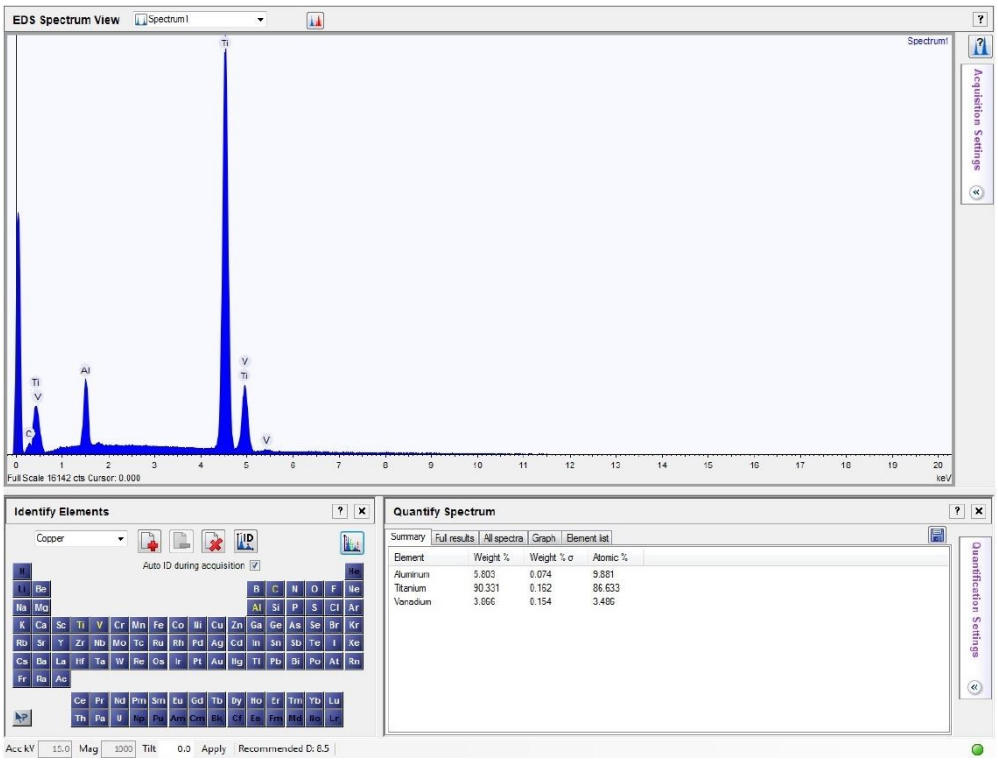

Figure 37: Ti6Al4V Job 8 chemical composition analysis at the edge of the specimen with EDX spectroscopy.

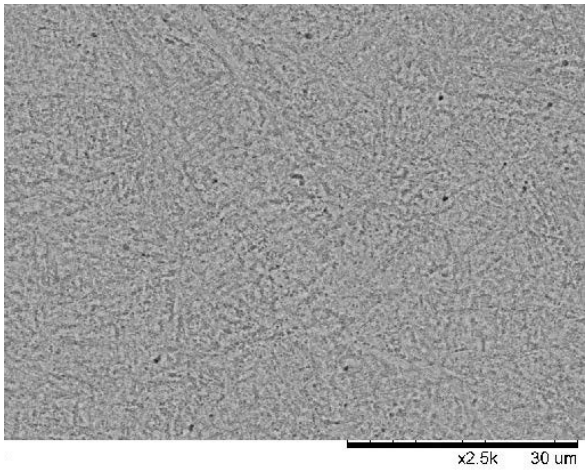

Figure 38: Ti6Al4V Job 8 microstructure at the center of the specimen - SEM image.

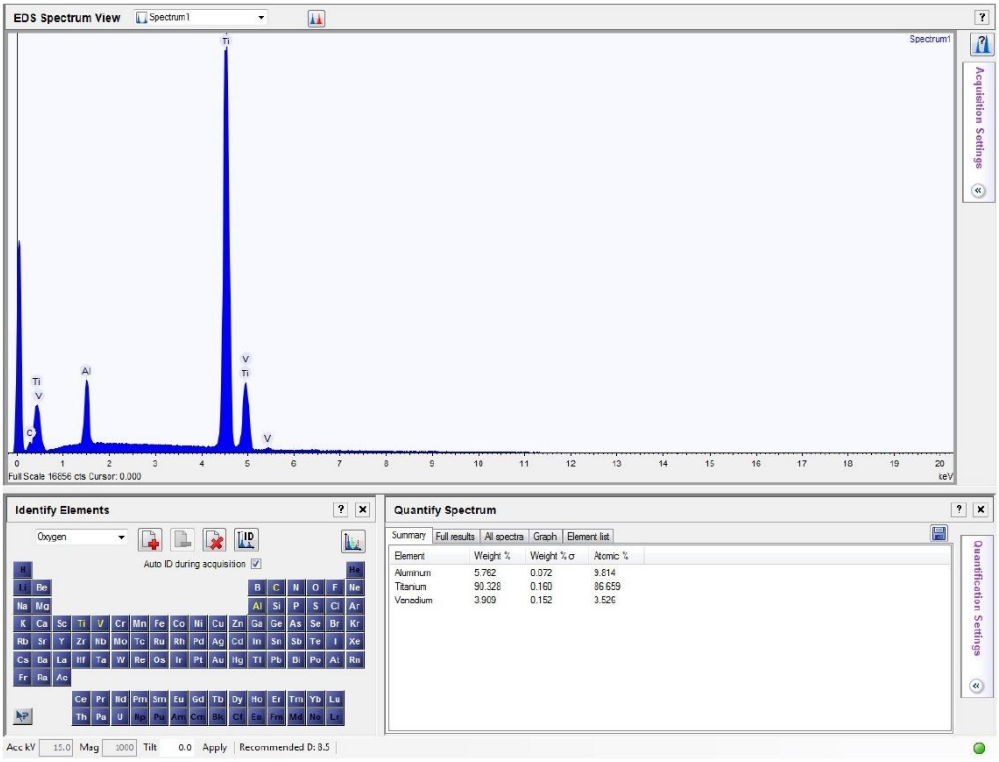

Figure 39: Ti6Al4V Job 8 chemical composition analysis at the center of the specimen with EDX spectroscopy.

During the investigation of microstructure and chemical composition of Job 8 a Fe precipitate has been found in a small region around the centre of the specimen (Fig. 40).

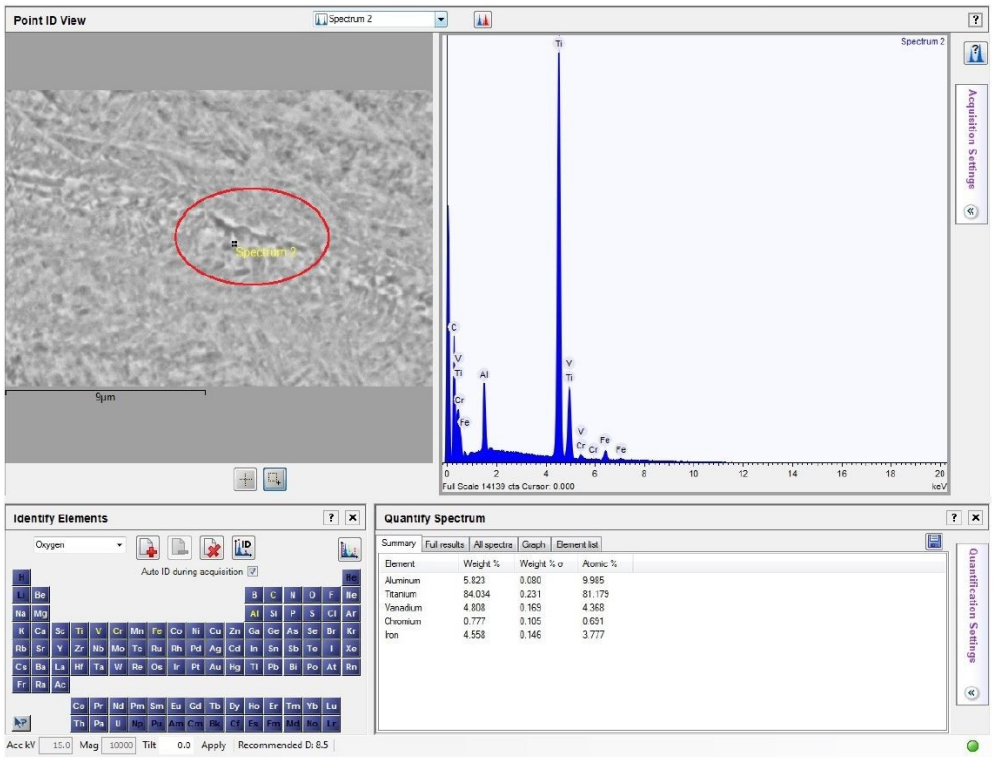

Figure 40: Chemical composition analysis of a small region around the centre of Job 8 using EDX spectroscopy.

The presence of Fe and Cr is a clear signal that a contamination occurred during the printed process. This result supports the idea that the last three jobs, i.e. Job 7,8 and 9, have been contaminated.

In order to explain the behaviour of the mechanical properties of the samples printed with reused powders the chemical composition of Job 0, 6 and 7 has been determined also using the coupled plasma mass spectroscopy (ICP). The results are summarized in Table 17. The increase of Fe, Cr and Ni content is an experimental proof that the contamination of Ti6Al4V powders during the printing process is caused by a stainless steel.

Table 17: Results of chemical analysis on tensile specimens of Job 0, 6 and 7.

	Job 0	Job 6	Job 7
Cr	0,005	0,006	0,037
Al	5,901	6,55	6,22
Fe	0,0189	0,219	0,4
Mn	0,005	0,006	0,007
Mg	0,199	0,217	0,164
Ni	0,002	0,002	0,01
Cu	0,011	0,012	0,017
Si	0,297	0,317	0,277
Mo	0,001	0,001	0,001
Na	0,035	0,039	0,034
Sn	0,002	0,007	0,007
Ti	86,85	86,83	84,44
V	<0,01	<0,01	<0,01

6.3 PH1

6.3.1 Powder analysis results

Chemical Analysis for PH1 powder are shown in Table 18 and plotted in Figure 41.

Table 18: PH1 chemical powders analysis

Results [%]										
	Job 0	**Job 1**	**Job 2**	**Job 3**	**Job 4**	**Job 5**	**Job 6**	**Job 7**	**Job 8**	**Job 9**
C	0,01	0,01	0,01	0,01	/	/	0,01	0,01	0,01	0,01
Cr	12,6	12,9	14,5	14,3	/	/	14,3	13,9	14,1	14,1
Al	0,04	<0,01	<0,01	0,02	/	/	0,01	<0,01	<0,01	<0,01
Fe	Rest	Rest	Rest	Rest	/	/	Rest	Rest	Rest	Rest
Mn	0,05	0,05	0,06	0,06	/	/	0,05	0,05	0,06	0,06
Mo	0,02	0,02	0,02	0,02	/	/	0,02	0,02	0,02	0,02
Ni	3,5	3,6	4,1	4,0	/	/	3,9	3,9	3,9	3,9
Cu	2,9	3,0	3,4	3,5	/	/	3,3	3,3	3,3	3,3
Si	0,44	0,40	0,46	0,45	/	/	0,47	0,44	0,45	0,44
P	0,007	0,007	0,008	0,007	/	/	0,008	0,008	0,008	0,007
N	0,06	0,06	0,06	0,05	/	/	0,05	0,05	0,05	0,06
Ti	<0,01	<0,01	<0,01	<0,01	/	/	<0,01	<0,01	<0,01	<0,01
V	0,02	0,01	0,02	0,02	/	/	0,02	0,02	0,02	0,02
S	0,005	0,005	0,005	0,005	/	/	0,005	0,005	0,005	0,005
H	0,0006	0,0006	0,0006	0,0005	/	/	0,0005	0,0005	0,0006	0,0006
Co	0,02	0,02	0,02	0,02	/	/	0,02	0,02	0,02	0,02

Please note that two powder specimens of PH1 alloy have been lost during tests (Job 4 and 5). Chemical results are therefore available for eight PH1 specimens families only.

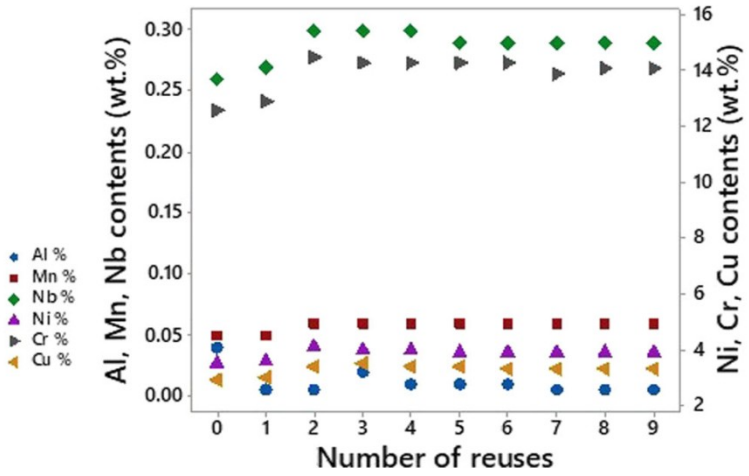

Figure 41: Chemical PH1 powder composition versus reuse times

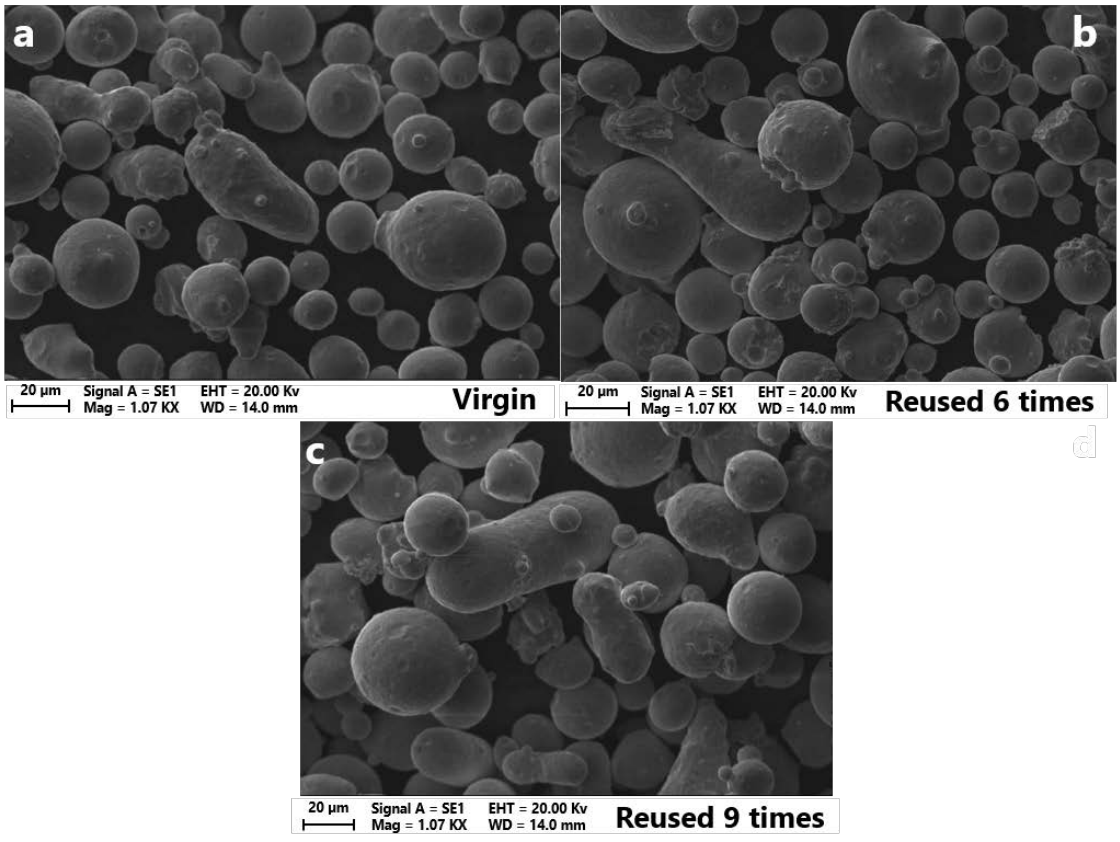

Figure 42: SEM images of the PH1 powder:

a) Virgin. b) Reused 6 times. c) Reused 9 times

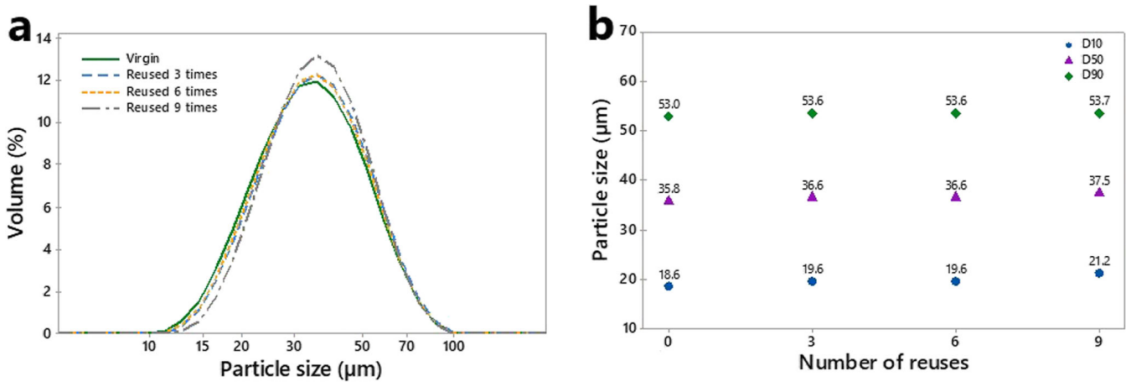

Figure 43: Particle size distribution of the PH1 powder over number of reuses. a) Volumetric percentage of particle size. b) D10, D50 and D90 of particle size

Table 19: Mean value, 10th (*D*10), 50th (*D*50) and 90th (*D*90) percentiles of PH1 particle diameter

Results			
Number of reuses	***D10 [µm]***	***D50 [µm]***	***D90 [µm]***
0	21,2	35,9	59,9
1	22,1	36,7	59,91
2	22,1	39,2	66,3
3	22,0	37,0	61,2
4	/	/	/
5	/	/	/
6	21,8	36,7	60,6
7	19,8	34,7	60,3
8	22,9	38,2	62,7
9	23,2	37,7	60,5

Table 20: Tap density and apparent density of the PH1 powder over number of reuses

Number of reuses	*Apparent Density [g/cm^3]*	*Tap Density [g/cm^3]*
0	4,04	4,60
1	4,04	4,56
2	4,09	4,57
3	4,03	4,49
4	/	/
5	/	/
6	4,18	4,64
7	4,20	4,61
8	4,23	4,78
9	4,17	4,77

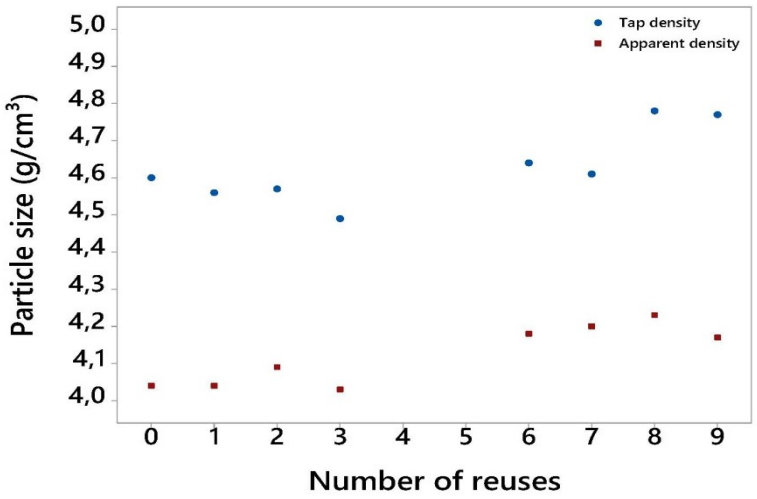

Figure 44: Tap density and apparent density of the PH1 powder over number of reuses

As shown in Fig. 41, 42, 43 and 44, elemental composition, tap density and apparent density of the reused PH1 powder remained substantially constant over the number of reuses.

Figure 43a shows a progressive rightward shift of PSDs with increasing number of reuses for PH1 powder, indicating a gradual reduction of smaller particles fraction.

Figure 43b shows the values of 10th (D10), 50th (D50) and 90th (D90) percentiles of the particle diameter corresponding to the curve represented in Fig. 42a, under the assumption of log-normal distribution. This latter was identified as the most suitable to depict the observed PSDs through the Anderson-Darling test [43, 44]. The test was carried out with $\alpha = 0.05$ by the Minitab 19 statistical software. Particle shape exhibited a deviation from the normal spherical one, with the presence of oval shaped particles and aggregates, as it can be seen from SEM images of virgin and reused powder presented in Fig. 42.

6.3.2 Mechanical test results

The Minitab 19 software was also used to perform the one-way analysis of variance (ANOVA), with $\alpha = 0.05$, on tensile properties. Before proceeding with the analysis, diagnostic check of residuals and removal of detected outliers were performed. Downstream of statistical analysis, the effect of number of reuses undergone by the powder can be declared as statistically significant on the observed variability of mechanical properties if the calculated *p*-values result lower than the selected significance level, α . ANOVA results for yield strength, *YS 0.2%*, ultimate tensile strength, *UTS*, and elongation at break, *A*, of PH1 are reported in Table 21.

Table 21: One-way ANOVA results for the effect of number of reuses on stainless steel PH1

Variable	Source	DOF	Adj SS	*f*-value	*p*-value
YS0.2%	Number of reuses	9	10316	1.54	0.162
	Error	49	36562		
	Total	58			
UTS	Number of reuses	9	806.4	1.12	0.365
	Error	50	3990.9		
	Total	59			
A	Number of reuses	9	20.49	3.88	0.001
	Error	49	28.74		
	Total	58			

The effect of number of reuses resulted statistically significant only on elongation at break.

Figure 44 shows the trends of the mechanical properties over the number of reuses.

In particular, Figs. 45c and 46 show the decrease of PH1 ductility over number of reuses.

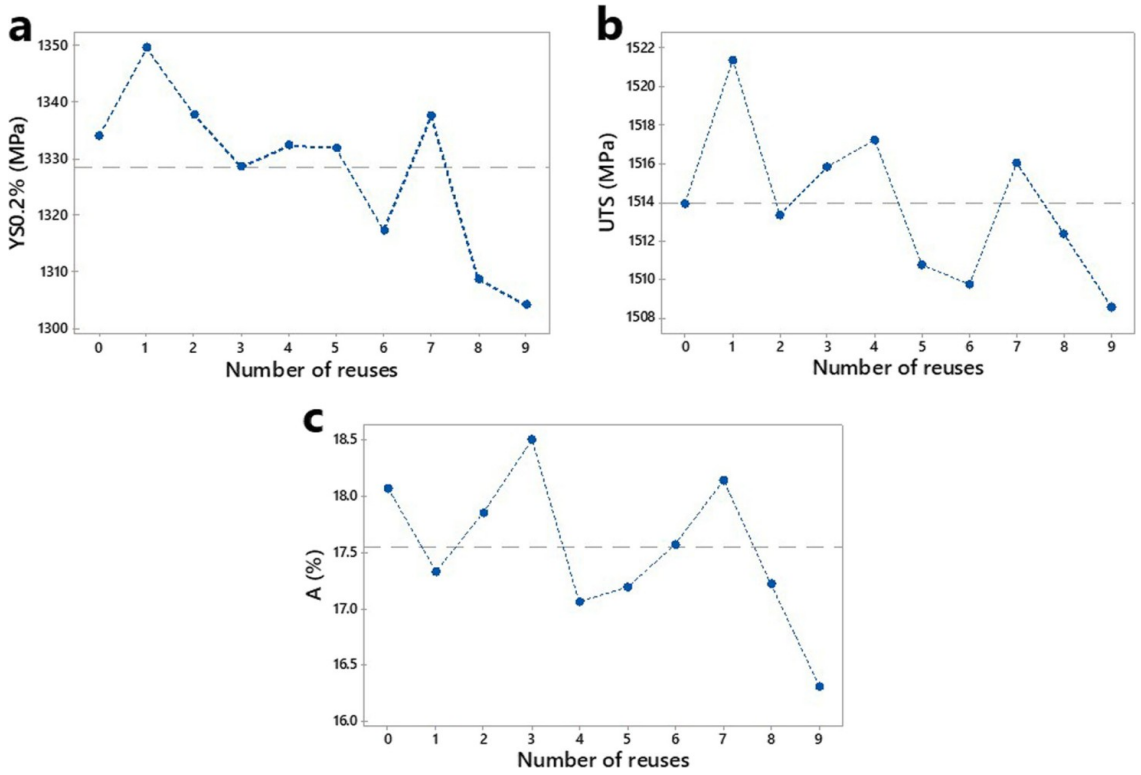

Figure 45: Main Effects Plots for the effect of number of reuses on PH1 tensile properties.

a) Yield strength. b) Ultimate tensile strength. c) Elongation at break

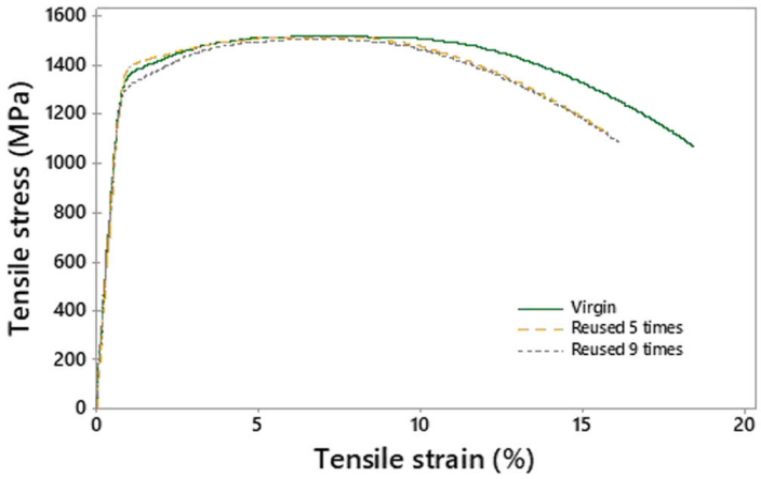

Figure 46: Stress-strain curves of PH1 samples produced with virgin and reused powder

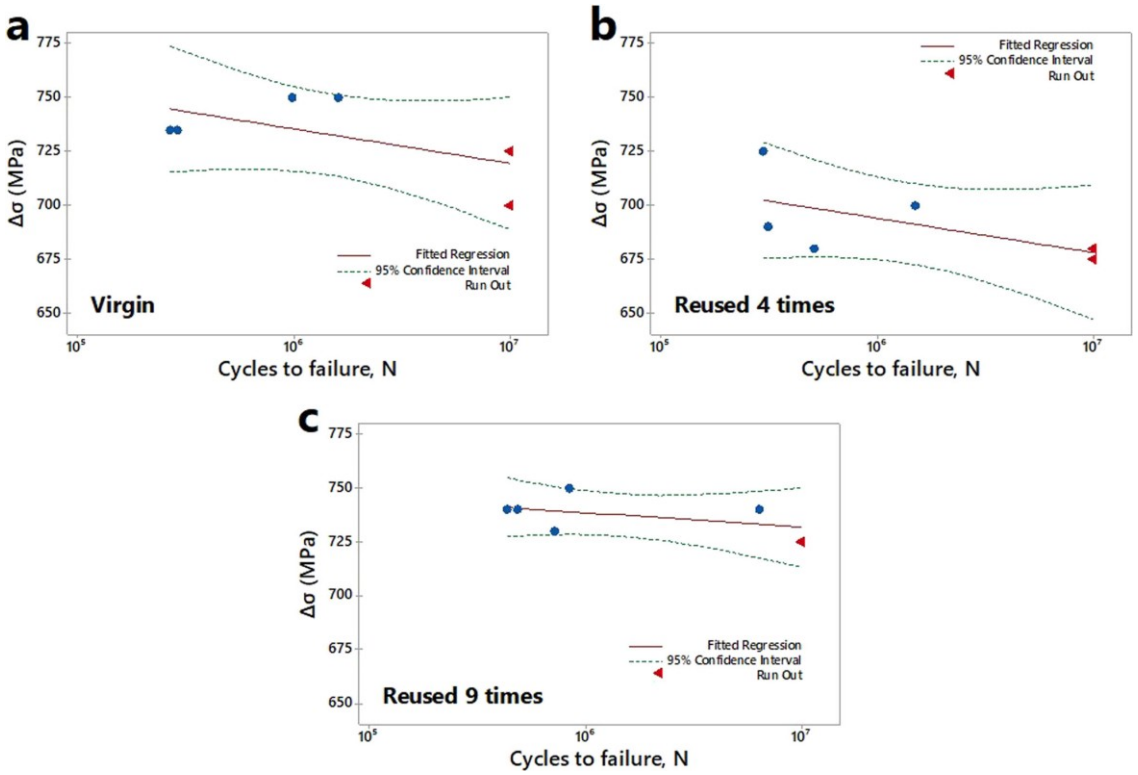

Figure 47: Wohler curves of the PH1 HCF samples produced with virgin and reused powder. a) Virgin. b) Reused 4 times. c) Reused 9 times

Figure 47 show the Wohler curves of specimens produced with virgin and reused powder. The fatigue behaviour remained substantially stable, with minimum high cycle fatigue strengths ($\Delta\sigma$) of 675 MPa.

6.4 GP1

6.4.1 Powder analysis results

Chemical Analysis for GP1 powder are shown in Table 22 and plotted in Figure 48.

Table 22: GP1 chemical powders analysis

Results [%]										
	Job 0	**Job 1**	**Job 2**	**Job 3**	**Job 4**	**Job 5**	**Job 6**	**Job 7**	**Job 8**	**Job 9**
C	0,06	0,05	0,05	0,05	0,06	0,05	0,05	0,05	0,04	0,04
Cr	17,2	15,1	15,0	15,3	15,0	15,0	15,2	15,9	15,1	15,2
Al	<0,01	0,01	<0,01	0,01	<0,01	<0,01	<0,01	0,02	0,01	<0,01
Fe	Rest	Rest	Rest	Rest	Rest	Rest	Rest	Rest	Rest	Rest
Mn	0,75	0,55	0,51	0,52	0,49	0,54	0,54	0,58	0,40	0,41
Mo	0,03	0,07	0,09	0,10	0,10	0,08	0,08	0,07	0,05	0,06
Ni	4,5	3,9	3,9	4,0	3,9	3,9	3,9	4,1	3,8	4,0
Cu	4,4	4,0	4,0	3,9	3,8	3,8	3,7	4,0	3,9	3,8
Si	0,58	0,55	0,56	0,63	0,56	0,56	0,57	0,61	0,52	0,55
P	0,013	0,013	0,018	0,013	0,014	0,013	0,013	0,014	0,012	0,013
N	0,02	0,03	0,03	0,03	0,03	0,03	0,03	0,03	0,03	0,03
Ti	0,14	0,15	0,15	0,15	0,15	0,15	0,15	0,15	0,12	0,12
V	<0,01	<0,01	<0,01	<0,01	<0,01	<0,01	<0,01	<0,01	<0,01	<0,01
S	0,03	0,02	0,02	0,02	0,02	0,01	0,01	0,03	0,02	0,02
H	0,009	0,008	0,007	0,007	0,007	0,008	0,008	0,008	0,007	0,007
Co	0,0006	0,0007	0,0008	0,0005	0,0005	0,0008	0,0008	0,0005	0,0006	0,0013

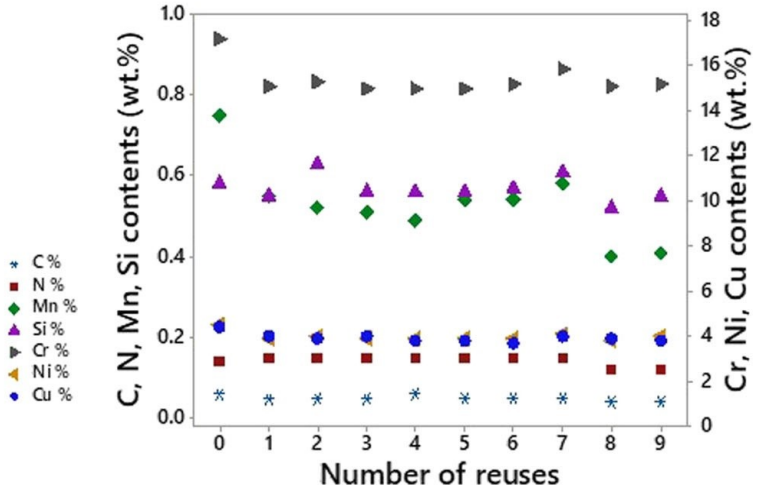

Figure 48: Chemical GP1 powder composition versus reuse times

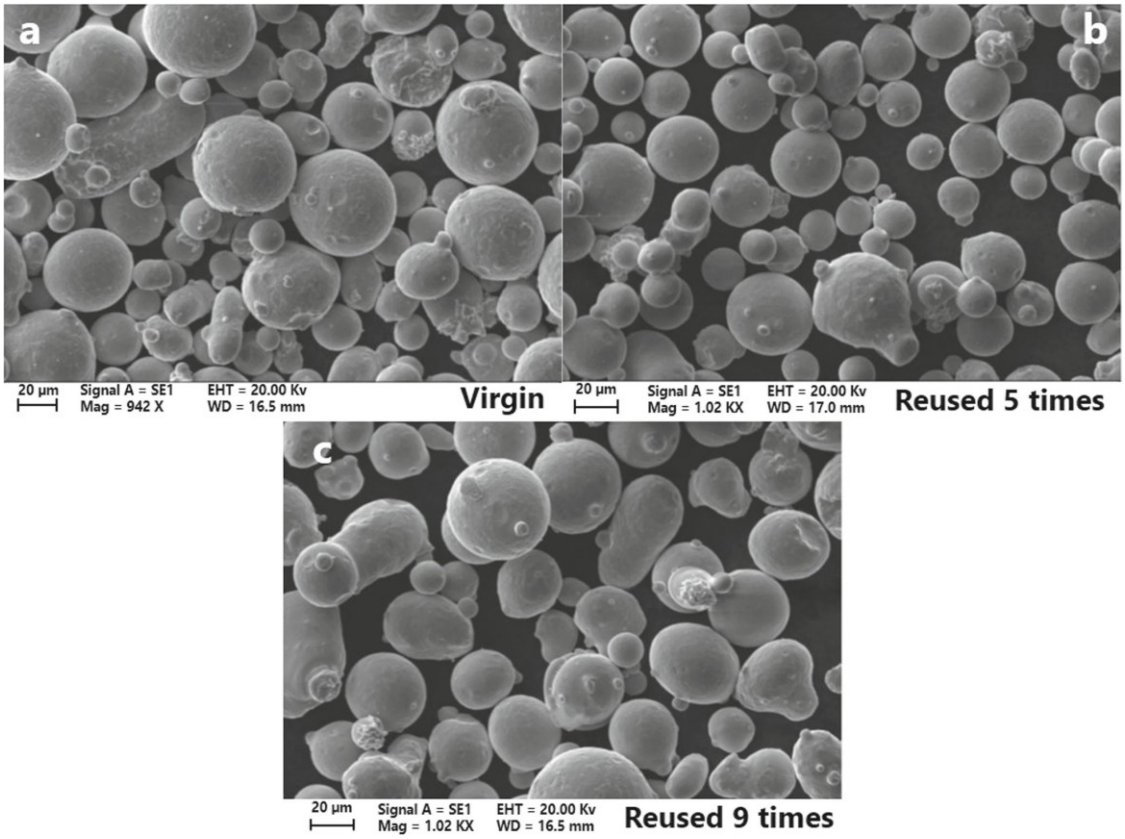

Figure 49: SEM images of the GP1 powder.
a) Virgin. b) Reused 5 times. c) Reused 9 times

Table 23: Mean value, 10th (*D*10), 50th (*D*50) and 90th (*D*90) percentiles of GP1 particle diameter

Results			
Number of reuses	***D10* [µm]**	***D50* [µm]**	***D90* [µm]**
0	22,4	38,8	65,5
1	21,2	36,1	60,9
2	22,3	37,0	60,6
3	23,4	38,3	62,3
4	23,8	38,9	62,9
5	19,2	33,4	58,4
6	21,0	36,0	60,1
7	19,6	33,8	57,9
8	19,4	34,0	60,6
9	24,0	39,4	64,3

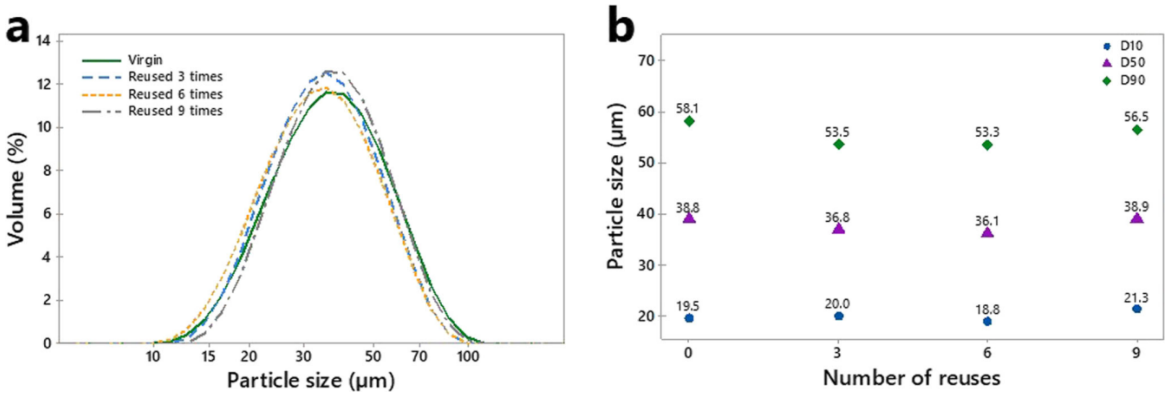

Figure 50: Particle size distribution of the GP1 powder over number of reuses. a) Volumetric percentage of particle size. b) *D*10, *D*50 and *D*90 of particle size.

The variability of GP1 PSDs can be considered substantially physiological, as shown in Fig. 50.

Table 24: Tap density and apparent density of the GP1 powder over number of reuses

Number of reuses	*Apparent Density [g/cm³]*	*Tap Density [g/cm³]*
0	4,25	4,68
1	4,17	4,70
2	4,22	4,73
3	4,22	4,67
4	4,18	4,69
5	4,23	4,66
6	4,21	4,68
7	4,23	4,78
8	4,21	4,64
9	4,17	4,75

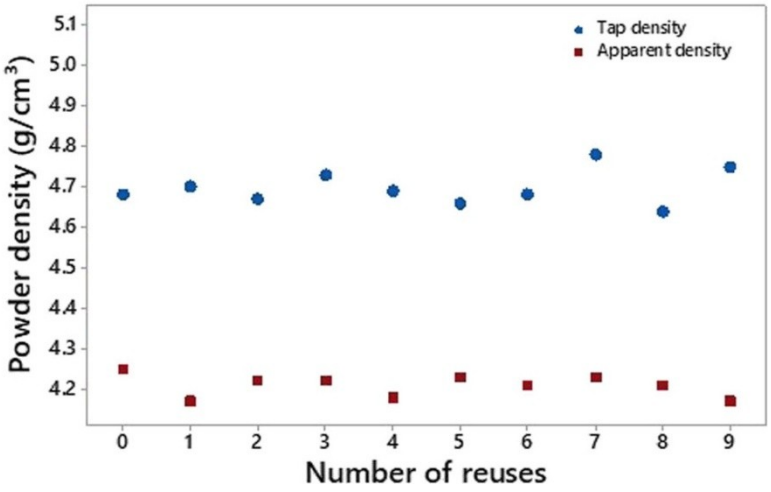

Figure 51: Tap density and apparent density of the GP1 powder over number of reuses

Figure 50b shows the values of 10th (D10), 50th (D50) and 90th (D90) percentiles of the particle diameter corresponding to the curve represented in Fig. 50a, under the assumption of log-normal distribution. This latter was identified as the most suitable to depict the observed PSDs through the Anderson-Darling test [43, 44]. The test was

carried out with $\alpha = 0.05$ by the Minitab 19 statistical software. Particle shape exhibited a deviation from the normal spherical one, with the presence of oval shaped particles and aggregates, as it can be seen from SEM images of virgin and reused powder presented in Fig. 49.

6.4.2 Mechanical tests results

The Minitab 19 software was also used to perform the one-way analysis of variance (ANOVA), with $\alpha = 0.05$, on tensile properties. Before proceeding with the analysis, diagnostic check of residuals and removal of detected outliers were performed. Downstream of statistical analysis, the effect of number of reuses undergone by the powder can be declared as statistically significant on the observed variability of mechanical properties if the calculated *p*-values result lower than the selected significance level, α . ANOVA results for yield strength, *YS 0.2%*, ultimate tensile strength, *UTS*, and elongation at break, *A*, of GP1 are reported in Table 25.

Statistical analysis always returned *p*-values far lower than α, pointing out a significant effect of powder reuse.

Looking at Fig. 52, it can be seen how most of the variability of GP1 tensile characteristics is limited, especially for yield strength and elongation at break, to the last two DMLS runs. ANOVA results are confirmed by the shape of stress-strain curves over number of reuses, as shown in Fig. 53.

Table 25: One-way ANOVA results for the effect of number of reuses on stainless steel GP1

Variable	Source	DOF	Adj SS	*f*-value	*p*-value
YS0.2%	Number of reuses	9	352517	616.10	0.000
	Error	47	2988		
	Total	56			
UTS	Number of reuses	9	22629	67.63	0.000
	Error	45	1673		
	Total	54			
A	Number of reuses	9	483.32	56.45	0.000
	Error	49	46.61		
	Total	58			

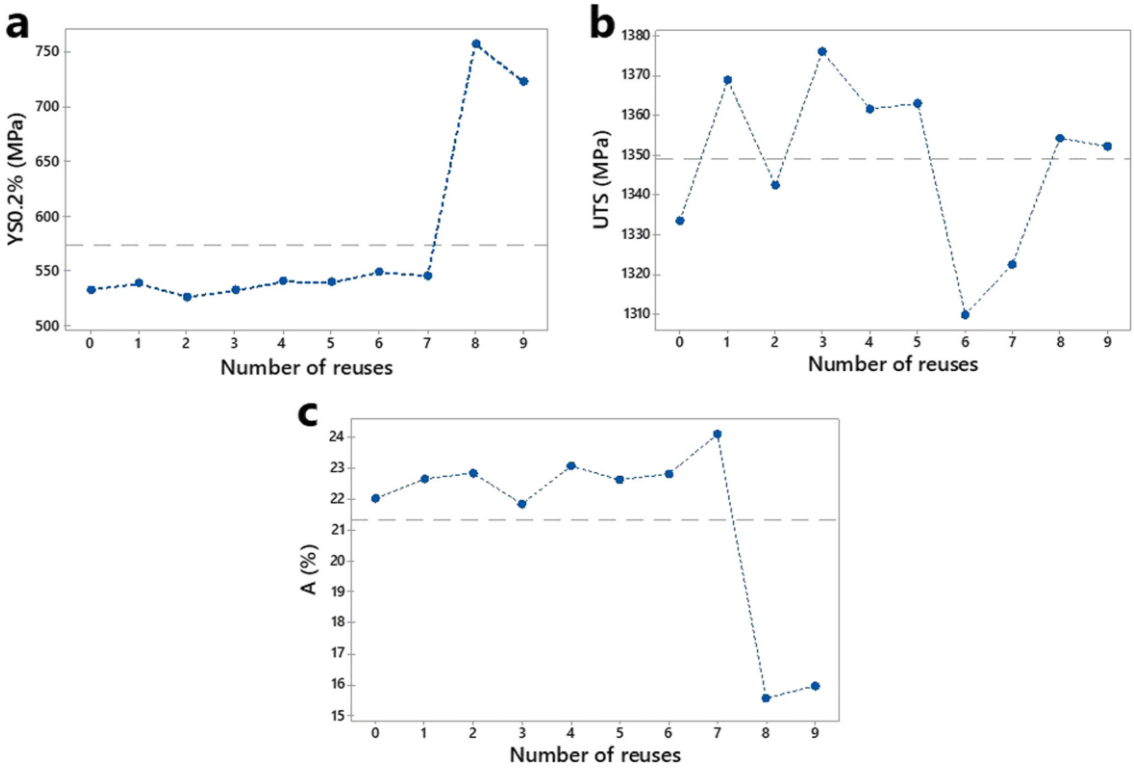

Figure 52: Main Effects Plots for the effect of number of reuses on GP1 tensile properties.

a) Yield strength. b) Ultimate tensile strength. c) Elongation at break

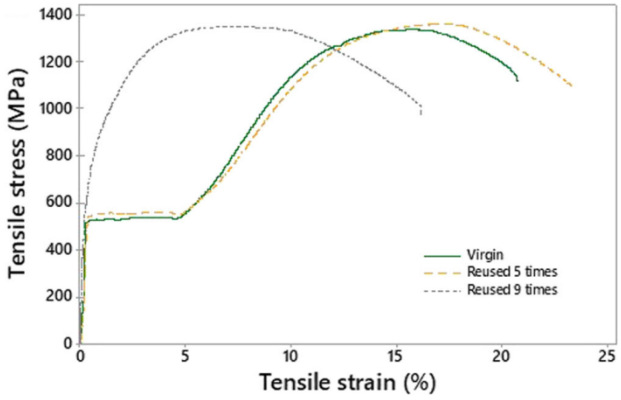

Figure 53: Stress-strain curves of GP1 samples produced with virgin and reused powder

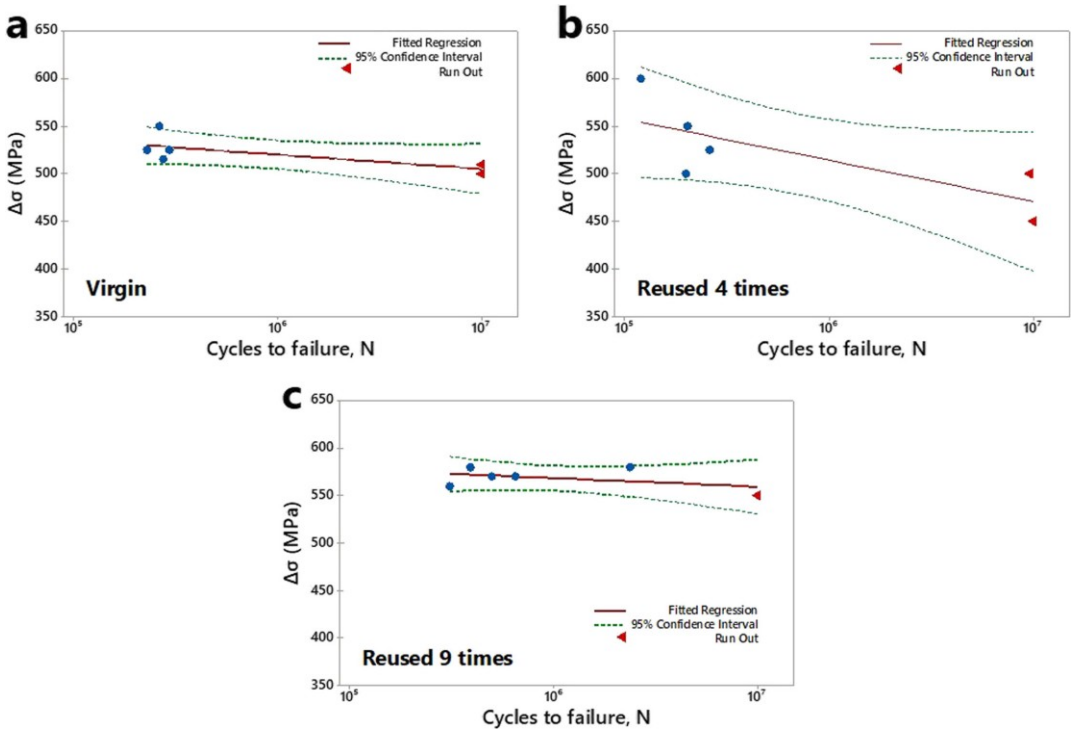

Figure 54: Wohler curves of the GP1 HCF samples produced with virgin and reused powder. a) Virgin. b) Reused 4 times. c) Reused 9 times

Figure 54 shows the Wohler curves of specimens produced with virgin and reused powder. The fatigue behaviour remained substantially stable, with minimum high cycle fatigue strengths ($\Delta\sigma$) of 450 MPa.

6.4.3 Technological investigation

Figures 52 and 53 highlight the abnormal behaviour, in terms of mechanical properties, of the GP1 specimens produced within the last two runs (stress-strain curves for runs 8 and 9 were nearly superimposable).

Due to their peculiar behaviour, specimens belonging to GP1 Job 0, 7, 8 and 9 have been selected in order to identify and study their microstructure. Job 7 is the last Job to show an expected behaviour during tensile tests, while Job 8 and Job 9 showed an unexpected behaviour during the same tests.

In addition, Figs. 55 and 56 show the fracture surfaces of specimens produced with virgin and reused powder, for PH1 and GP1, respectively. A thin section of specimens has been cut from one of the two specimen's extremity and then polished with different degree of polishing paper. Once a mirror finishing has been obtained, specimens have been treated with Vilella's Reagent (Picric acid 1g, Hydrochloric acid 5ml, Ethanol 100ml), in order to magnify alloys microstructure.

The abnormal mechanical properties of GP1 samples produced with powder reused eight and nine times are ascribable to the presence of a different microstructure, as shown in Figs. 57 and 58, obtained by optical microscopy (OM) and SEM, respectively. The absence of retained austenite in GP1 samples produced within the last two runs is clearly visible.

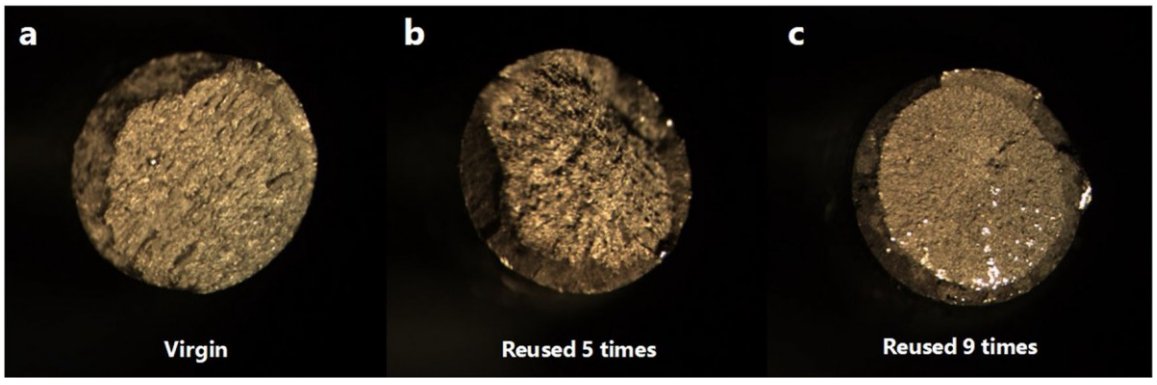

Figure 55: Fracture surfaces of the GP1 tensile samples produced with virgin and reused powder. a) Virgin. b) Reused 5 times. c) Reused 9 times

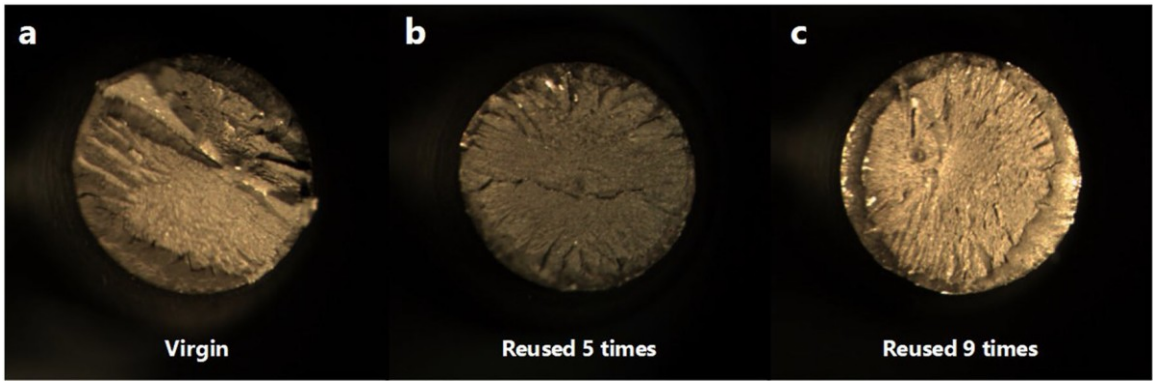

Figure 56: Fracture surfaces of the PH1 tensile samples produced with virgin and reused powder. a) Virgin. b) Reused 5 times. c) Reused 9 times

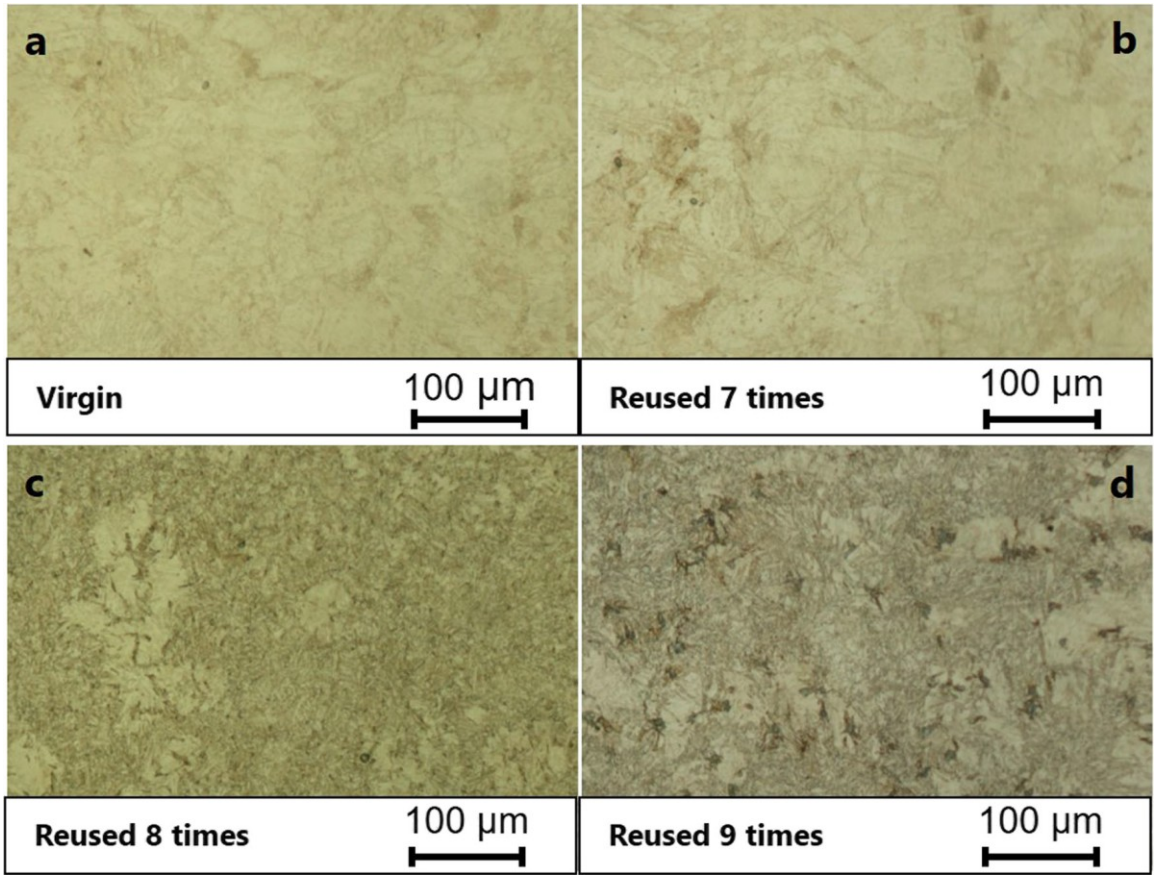

Figure 57: OM images GP1 samples microstructure. a) Virgin. b) Reused 7 times. c) Reused 8 times. d) Reused 9 times

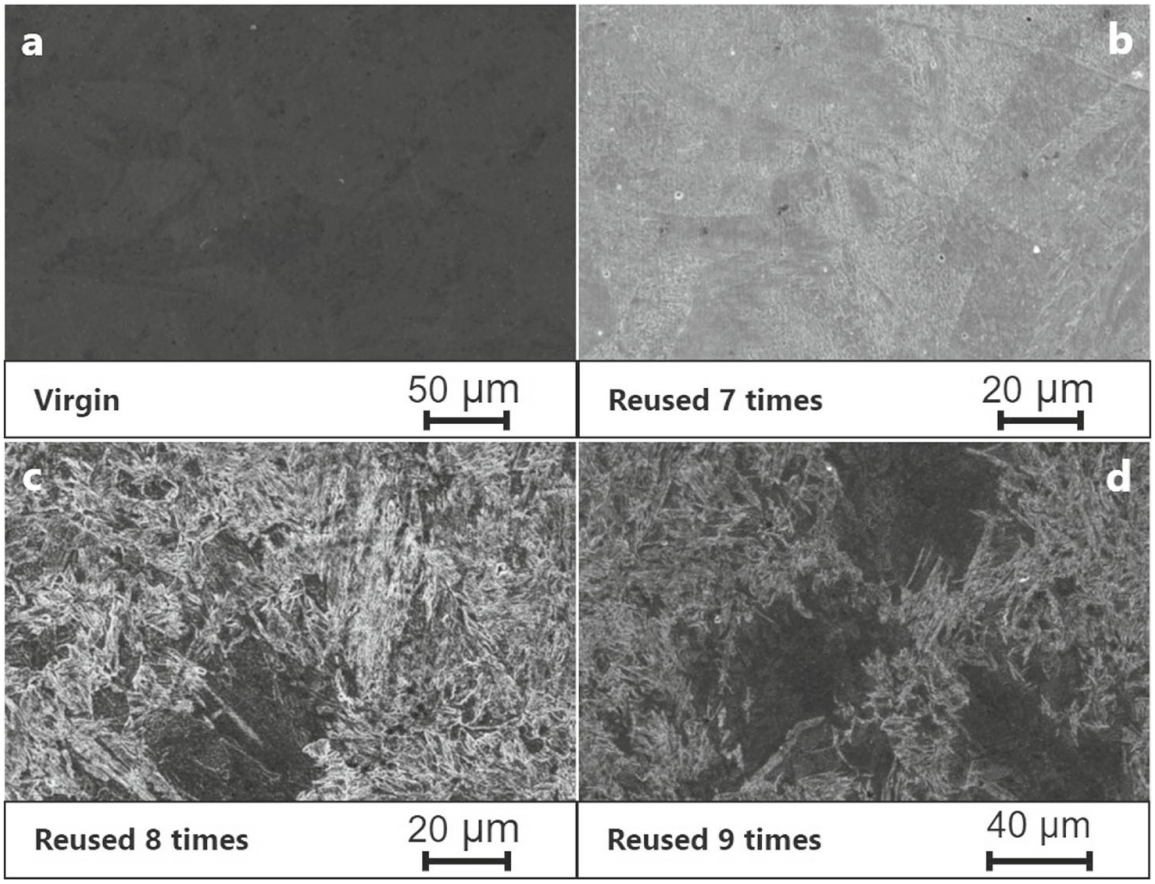

Figure 58: SEM images GP1 samples microstructure. a) Virgin. b) Reused 7 times. c) Reused 8 times. d) Reused 9 times

In order to explain the observed structure modification of GP1, the attention was focused on powder chemical composition that had exhibited, as aforementioned, some questionable anomalies. For both PH1 and GP1, further chemical analyses were performed on all the collected powder samples (Table 18 and 22), as well as on three additional ones of virgin powder, coming from other batches, to be considered a reference. A common practice in welding applications is to use the Schaeffler diagram to predict microstructure and δ- ferrite content of stainless steel weld metals [45]. Due to the similarity of welding and L-PBF techniques, which are both characterised by rapid cooling during the process, this diagram has proved very effective also in the latter [46] and was therefore used to understand the causes of the anomalous behaviour of GP1.

Figure 59 shows the final version of the graph proposed by Schaeffler himself in 1949 [47], while in Fig. 60, the diagram obtained for PH1 and GP1 powders is reported. The position of GP1 samples corresponding to the last two runs, highlighted by the red circle,

shows how the loss of retained austenite within GP1 is caused by phase transition of metal powder, due to the variation of Cr- and Ni-equivalents.

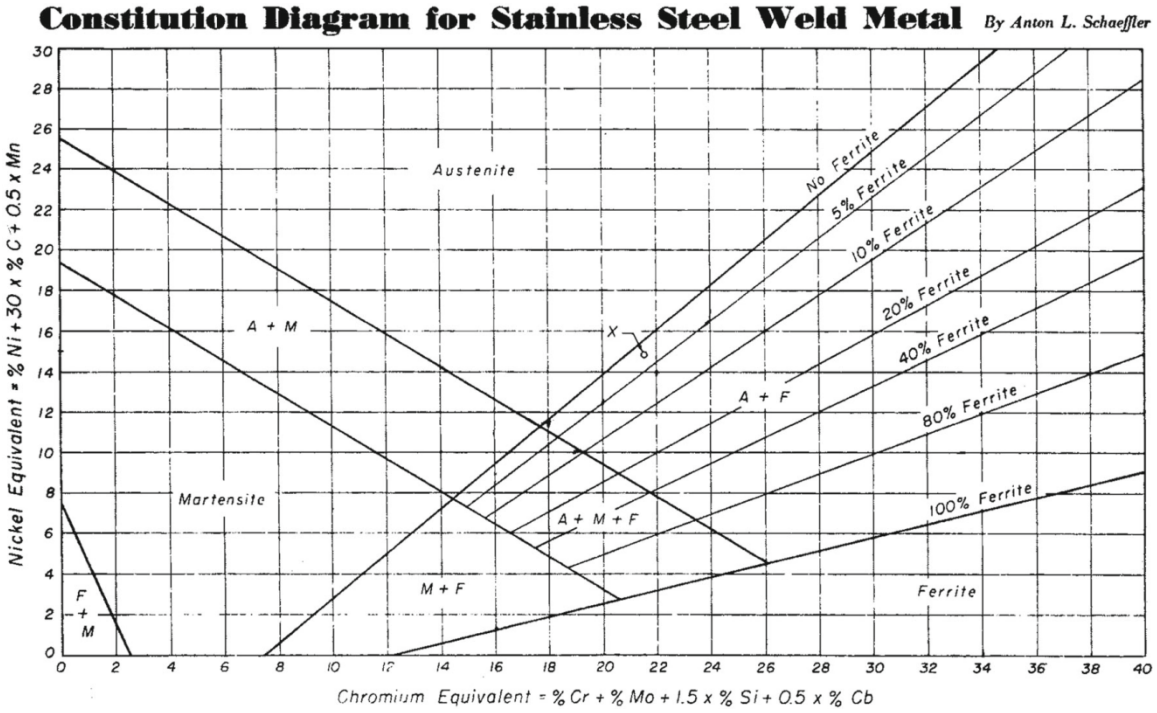

Figure 59: Final Schaeffler diagram for welding applications on stainless steels

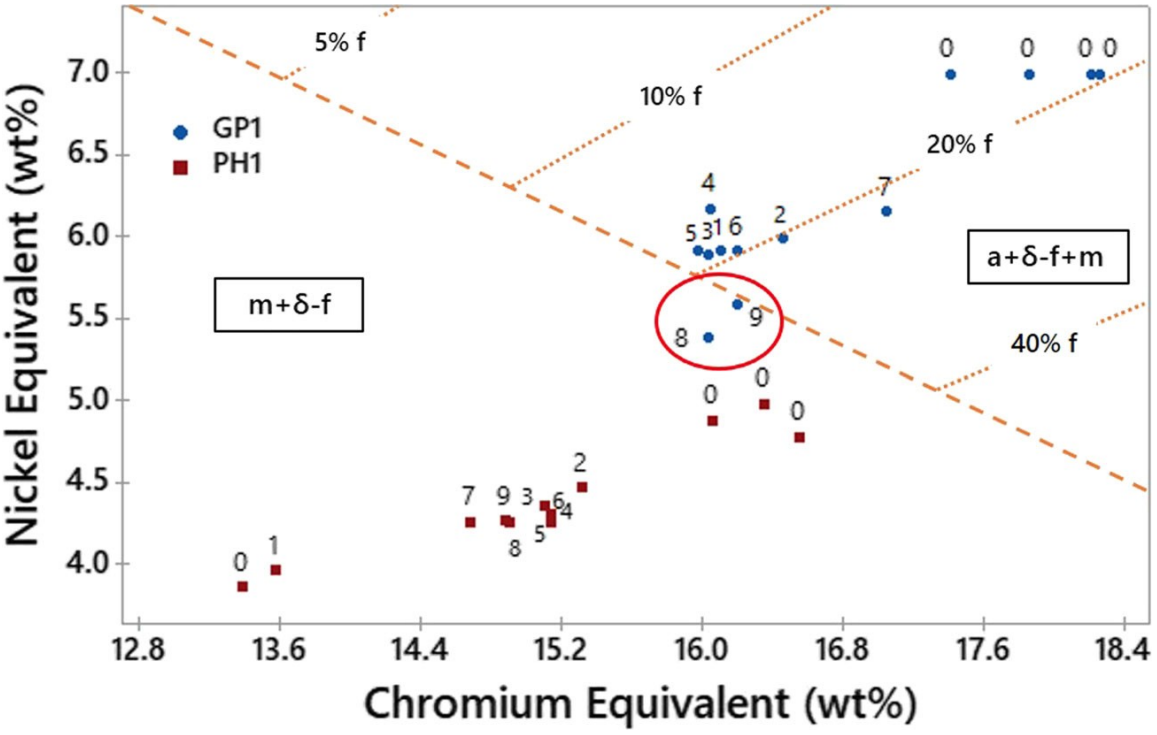

Figure 60: Schaeffler diagram of PH1 and GP1 for virgin (0) and reused (1 to 9) powder

CONCLUSIONS AND FUTURE WORK

The ANOVA results allowed to assess the statistical significance of powder reuse on the achievable mechanical properties of:

- EOS Aluminium AlSi10Mg parts
- EOS Titanium Ti64 parts
- EOS Stainless Steel GP1 parts
- EOS Stainless Steel PH1 parts

produced by DMLS technology.

AlSi10Mg alloy processed according to the experimental conditions shows statistical significance of powder reuse on yield strength and ultimate strength.
Despite the slight observed decrease of the final part features, it is worth noting that all the measured characteristics, included the fatigue resistance, resulted compliant with the company requirements.
It is necessary to underline that the recycling strategy 1 was used for this alloy.
This recycling strategy was not considered industrially convenient from the company because it implied to mix used powder, from the powder overflow container and the building platform, with the virgin one, stored in the dispenser.
A more industrial recycling strategy (recycling strategy 2) was used to assess the effects of recycling process on mechanical properties of the last three alloys, that involve only the powders on the *powder overflow container* and *building platform.*
Further studies should be done to assess the effect of using recycling strategy 2 on AlSi10Mg parts.

Ti6Al4V alloy processed according to the experimental conditions shows statistical significance of powder reuse on yield strength and ultimate strength.
These results are affected by the increase of iron content in Ti6Al4V powders after the seventh reuse. In particular, the increase of iron content raises yield and ultimate strength of Ti6Al4V specimens. It is worth noting that the percentage of iron is still acceptable for all the specimens because its values fall into the standards of ASTM B265-15. Other investigations have been carried out in order to explain the reason of this iron increase.

The results suggest that a contamination occurred during the printing process. In particular, the chemical composition analysis of Job 7 shows also a small increase of Chromium and Nickel percentages, proving that the contaminating material is a stainless steel.

Considering contaminated jobs as outliners, there is no statistical significance of powder reuse on Ti6Al4V mechanical properties.

All external procedures were correctly performed in accordance with protocols previously checked by MBDA during their research activities concerning the study of the properties of parts printed with a large variety of materials. The occurrence of an external contamination can be excluded. On the other hand, any internal component of the printing process can cause contaminations. In particular, the container and the sieve are made of stainless steel. Moreover, it is important to consider two features of the Ti6AL4V printing process: the first is that the hardness of Ti6Al4V is 50% higher than of stainless steel one and the second is that sieve and container, both made of stainless steel, are involved in collisions with powder. Thus, the occurrence of a stainless steel contamination could be explained taking account of the Ti6Al4V powders abrasivity. In particular, this explanation is in accordance with the causality of the increase of iron percentage in the chemical composition of Ti6Al4V powders starting from Job 7.

A possible solution can be the use of internal components, as sieve and container, with a Vickers hardness at least equal to that of Ti6Al4V alloys.

Further studies will be conducted to assess this hypothesis.

GP1 stainless steel processed according to the experimental conditions shows statistical significance of powder reuse on all mechanical properties analyzed.

The abnormal mechanical properties of GP1 samples produced with powder reused eight and nine times are ascribable to the presence of a different microstructure. This behaviour happened although experimental chemical compositional range of these two jobs are compliant to EOS datasheet for this alloy.

These results lead the company to discard the implementation of this alloy for its applications/products.

PH1 stainless steel processed according to the experimental conditions shows statistical significance of powder reuse only on elongation at break. This stainless steel showed great stability in terms of powder and mechanical properties.

REFERENCES

[1] eos.info (2013) *Additive manufacturing, laser-sintering and industrial 3D printing - benefits and functional principle*. http://www.eos.info/additive manufacturing/for technology interested

[2] Khaing MW, Fuh JYH, Lu L – *Direct metal laser sintering for rapid tooling: processing and characterization of EOS parts*. J Mater Process Technol - 2001

[3] Gardan J – *Additive manufacturing technologies: state of the art and trends*. Int J Prod Res – 2016

[4] Lutter-G¨unther M, Gebbe C, Camps T, Seidel C, Gunter R – *Powder recycling in laser beam melting: strategies, consumption modeling and influence on resource efficiency*. Prod Eng – 2016

[5] Sames WJ, List FA, Pannala S, Dehoff RR, Babu SS – *The metallurgy and processing science of metal additive manufacturing*. Int Mater Rev – 2016

[6] Slotwinski JA – *Materials standards for additive manufacturing*

lecture, Engineering Lab. NIST – 2013

[7] Scott J., Gupta N., Weber C., Newsome S., Wohlers T., Caffrey T. – *Additive Manufacturing: Status and Opportunities* – IDA Science and Technology Policy Institute – 2012

[8] Ford S.L.N. – *Additive Manufacturing Technology: Potential Implications for U. S. Manufacturing Competitiveness* – Journal of International Commerce and Economics – 2014

[9] Thomas D.S., Gilbert S.W. – *Costs and Cost Effectiveness of Additive Manufacturing – A Literature Review and Discussion* – NIST SP 1176 - 2014

[10] Ruffo M., Tuck C., Hague R.J.M. – *Cost Estimation for Rapid Manufacturing – Laser Sintering Production for Low to Medium Volumes* – Proceedings of the Institution of Mechanical Engineers, Part B: Journal of Engineering Manufacture – 2006

[11] Mohr S., Khan O. – *3D Printing and Supply Chains of the Future* – Proceedings of the Hamburg International Conference of Logistics (HICL) - 2015

[12] Morrow W.R., Qi H., Kim I., Mazumder J., Skerlos S.J. – *Environmental Aspects of Laser-Based and Conventional Tool and Die Manufacturing*- Journal of Cleaner Production - 2007

[13] Sreenivasan R., Bourell D.L. – *Sustainability Study in Selective Laser Sintering – An Energy Perspective* – 20th Annual International Solid Freeform Fabrication Symposium – An Additive Manufacturing Conference, Austin/TX/USA - 2009

[14] Bourell D.L., Leu M.C., Rosen D.W. – *Roadmap for Additive Manufacturing: Identifying the Future of Freeform Processing* – The University of Texas at Austin. Laboratory for Freeform Fabrication, Advanced Manufacturing Center – 2009

[15] NIST National Institute of Standards and Technology – *Measurement Science Roadmap for Metal-Based Additive Manufacturing* – NIST Workshop Summary Report – 2013

[16] Czitrom V. –*One-Factor-At-a-Time Versus Designed Experiments* – The American Statistician, Vol. 53, No. 2 - 1999

[17] Erto P. – *Probabilità e statistica per le scienze e l'ingegneria (3rd Ed.)* – McGraw-Hill Ed. - 2008

[18] Coleman D.E., Montgomery D.C. – *A Systematic Approach to Planning for a Designed Industrial Experiment* – Technometrics, Vol. 35, NO. 1 - 1993

[19] Montgomery D.C. –*Design and Analysis of Experiments* – John Wiley & Sons Inc. - 2001

[20] *EOS Aluminium AlSi10Mg for EOSINT M 270 – Material data sheet*

[21] *EOS Titanium Ti64 for EOSINT M 270 – Material data sheet*

[22] *EOS StainlessSteel PH1 for EOSINT M 270 – Material data sheet*

[23] *EOS StainlessSteel* GP1 *for EOSINT M 270 – Material data sheet*

[24] Ardila L.C., Garciandia F., González-Díaz J.B., Álvarez P., Echeverria A., Petite M.M., Deffley R., Ochoa J. – *Effect of IN718 recycled powder reuse on properties of parts manufactured by means of Selective Laser Melting* – 8th International Conference on Photonic Technologies - Physics Procedia 56 - 2014

[25] *Case study 05: Powder degradation of IN718 and Ti-6Al-4V* – LPW Technology - 2016

[26] Seyda V., Kaufmann N., Emmelmann C. - *Investigation of aging processes of Ti-6Al-4V powder material in laser melting* - Phys. Procedia -2012

[27] Tang H.P., Qian M., Liu N., Zhang X.Z., Yang G.Y., Wang J. – *Effect of powder reuse times on Additive Manufacturing of Ti-6Al-4V by Selective Electron Beam Melting* – Journal of the Minerals - 2015

[28] *Investigating the effects of multiple re-use of Ti6Al4V powder in Additive Manufacturing (AM)* – Whitepaper Renishaw -2016

[29] Slotwinski J.A., Garboczi E.J., Stutzman P.E., Ferraris C.F., Watson S.S., Peltz M.A. – *Characterization of metal powders used of Additive Manufacturing* – Journal of Research of the National Institute of Standards and Technology - 2014

[30] ASTM (2015) B215-15 standard practices for sampling metal powders. ASTM International

[31] Sutton AT, Kriewall CT, Leu MC, Newkirk JW – *Powder characterisation techniques and effects of powder characteristics on part properties in powder-bed fusion processes*. Virtual Phys Prototyp – 2017

[32] ASTM (2017) B822-17 standard test method for particle size distribution of metal powders and related compounds by lightscattering. ASTM International

[33] ASTM (2016) F1877-16 standard practice for characterization of particles. ASTM International

[34] ISO (2011) 3953:2011 metallic powders, determination of tap density. International Organization for Standardization. ICS 77.160

[35] ISO (2008) Standard 3923-1:2008 metallic powders, determination of apparent density, Part 1: funnel method. International Organization for standardization. ICS 77.160

[36] ASTM (2014) A751-14a standard test methods, practices, and terminology for chemical analysis of steel products. ASTM International

[37] ASTM (2014) E1019-11 standard test methods for determination of carbon, sulfur, nitrogen and oxygen in steel, iron, nickel, and cobalt alloys by various combustion and fusion techniques. ASTM International.

[38] EN ISO (2016) Standard 6892-1:2016 metallic materials, tensile testing, Part 1: method of test at room temperature. International Organization for Standardization. ICS 77.040.10

[39] DIN EN (2011) 6072:2011 Aerospace series, metallic materials, test methods, constant amplitude fatigue testing. German institute for Standardization

[40] ASTM (2016) E8/E8M-16a standard test methods for tension testing of metallic materials. ASTM International.

[41] ASTM (2015) E466-15 Standard practice for conducting force controlled constant amplitude axial fatigue tests of metallic materials. ASTM International

[42] ASTM (2015) E739-10 Standard practice for statistical analysis of linear or linearized stress-life (S-N) and strain-life (ε-N) fatigue data. ASTM International.

[43] Montgomery DC (2005) Design and analysis of experiments.

Wiley, Hoboken. ISBN 0-471-31649-0

[44] Montgomery DC, Runger GC – *Applied statistics and probability for engineers*. Wiley, Hoboken. ISBN – 2003

[45] Guiraldenq P, Duparc OH – *The genesis of the Schaeffler diagram in the history of stainless steel*. Metal Res Technol – 2017

[46] Jacob G – *Prediction of solidification phases in Cr-Ni stainless steel alloys manufactured by laser based powder bed fusion process*. NIST – 2018

[47] Schaeffler AL – *Constitution diagram for stainless steel weld metal*. Metal Progress – 1949